STATE UNIVERSITY OF PONTA GROSSA
PRO-RECTORY OF RESEARCH AND POSTGRADUATE
MASTER DEGREE PROGRAM IN ENVIRONMENTAL AND SANITARY ENGINEERING

FERNANDO ROBERTO DOS SANTOS

EFFECTS OF A FLOATING PHOTOVOLTAIC SYSTEM ON THE WATER EVAPORATION RATE IN THE PASSAÚNA RESERVOIR
EFEITOS DE UM SISTEMA FOTOVOLTAICO FLUTUANTE NA TAXA DE EVAPORAÇÃO DA ÁGUA DO RESERVATÓRIO DO PASSAÚNA

PONTA GROSSA
2022

FERNANDO ROBERTO DOS SANTOS

EFFECTS OF A FLOATING PHOTOVOLTAIC SYSTEM ON THE WATER EVAPORATION RATE IN THE PASSAÚNA RESERVOIR

EFEITOS DE UM SISTEMA FOTOVOLTAICO FLUTUANTE NA TAXA DE EVAPORAÇÃO DA ÁGUA DO RESERVATÓRIO DO PASSAÚNA

Dissertation submitted to the Master Degree Program in Environmental and Sanitary Engineering of the State University of Ponta Grossa as a requirement for obtaining the title of Master.

Advisor: Prof. Dr. Giovana Kátie Wiecheteck

Co-advisor: Prof. Dr. Jorim Sousa das Virgens Filho

PONTA GROSSA

2022

Santos, Fernando Roberto dos
S237 Effects of a floating photovoltaic system on the water evaporation in the Passaúna reservoir / Fernando Roberto dos Santos. Ponta Grossa, 2022.
84 f.

Dissertação (Mestrado em Engenharia Sanitária e Ambiental - Área de Concentração: Saneamento Ambiental e Recursos Hídricos), Universidade Estadual de Ponta Grossa.

Orientadora: Profa. Dra. Giovana Kátie Wiecheteck.
Coorientador: Prof. Dr. Jorim Sousa das Virgens Filho.

1. Water evaporation. 2. Floating photovoltaic system. 3. Climate change. I. Wiecheteck, Giovana Kátie. II. Virgens Filho, Jorim Sousa das. III. Universidade Estadual de Ponta Grossa. Saneamento Ambiental e Recursos Hídricos. IV.T.

CDD: 628.4

Ficha catalográfica elaborada por Maria Luzia Fernandes Bertholino dos Santos- CRB9/986

CERTIFICADO DE APROVAÇÃO - DISSERTAÇÃO DE MESTRADO

PROGRAMA DE PÓS-GRADUAÇÃO EM ENGENHARIA SANITÁRIA E AMBIENTAL
Certificado nº 01/2022 PPGESA

Título da Dissertação: "**EFFECTS OF A FLOATING PHOTOVOLTAIC SYSTEM ON THE WATER EVAPORATION RATE IN THE PASSAÚNA RESERVOIR**".

Nome: FERNANDO ROBERTO DOS SANTOS

Orientadora: Profª. Drª. Giovana Kátie Wiecheteck

Co-orientador: Prof. Dr. Jorim Sousa das Virgens Filho

Aprovado pela Comissão Examinadora:

Profª. Drª. Giovana Kátie Wiecheteck
Universidade Estadual de Ponta Grossa/Ponta Grossa - PR

Prof. Dr. Terrence Chambers
University of Louisiana at Lafayette/Lafayette – Louisiana (EUA)

Prof. Dr. Gabriel Alfredo Carranza
University of Louisiana at Lafayette/Lafayette – Louisiana (EUA)

Ponta Grossa, 10 de junho de 2022.

Documento assinado eletronicamente por **Giovana Katie Wiecheteck**, **Coordenador(a) do Programa de Pós-Graduação em Engenharia Sanitária e Ambiental - Mestrado**, em 14/06/2022, às 15:16, conforme Resolução UEPG CA 114/2018 e art. 1º, III, "b", da Lei 11.419/2006.

Documento assinado eletronicamente por **Gabriel A. Carranza**, **Usuário Externo**, em 14/06/2022, às 17:58, conforme Resolução UEPG CA 114/2018 e art. 1º, III, "b", da Lei 11.419/2006.

Documento assinado eletronicamente por **Terrence Chambers**, **Usuário Externo**, em 20/07/2022, às 17:14, conforme Resolução UEPG CA 114/2018 e art. 1º, III, "b", da Lei 11.419/2006.

A autenticidade do documento pode ser conferida no site https://sei.uepg.br/autenticidade informando o código verificador **1020042** e o código CRC **7D58470D**.

ACKNOWLEDGEMENTS

First and foremost, I would like to thank my family, especially my father and mother, for their support and encouragement in my studies.

To Dr. Giovana Kátie Wiecheteck for guiding me through this research. For the contribution of her knowledge, the orientation, and for challenging myself in this thesis.

To Dr. Jorim Sousa das Virgens Filho for accepting to be co-advisor of my work, for the contribution of his knowledge, and for his help in the development of this thesis.

To the professors of the Master Degree Program in Environmental and Sanitary Engineering of the State University of Ponta Grossa, for the knowledge and the new ways of thinking.

To the Water and Sanitation Company of Paraná State (SANEPAR) for the data and support, which were fundamental to develop this research.

To the State University of Ponta Grossa and to the Master Degree Program in Environmental and Sanitary Engineering for the opportunity to accomplish the master's degree and achievement of scientific knowledge.

To my colleagues of the Master Degree Program in Environmental and Sanitary Engineering, especially to Sauana, for the friendship in a year full of obstacles.

To my dearest friend Pedro for always believing in my potential.

To all who participated and contributed directly or indirectly to the achievement of this research.

And above all, to the triad, God, Mother, and Son.

"If I have seen further,
it is by standing upon the shoulders of giants."
(Isaac Newton)

ABSTRACT

Freshwater scarcity is a significant concern due to climate change in some regions of Brazil. Water evaporation rates in reservoirs increase with increasing temperatures, which can represent a great challenge for managing water resources. The coverage area of floating photovoltaic systems reduces the amount of sunlight on the water surface, reducing the water evaporation rates. In 2019 a floating photovoltaic system was installed in the Passaúna reservoir, located in the metropolitan region of Curitiba, State of Paraná, southern Brazil. The general objective of this work is to study the effects of the floating photovoltaic system in the Passaúna reservoir on water evaporation. Based on this objective, the work was divided into two chapters: in the first chapter, the evaporation avoided by the installation of the floating photovoltaic system in the Passaúna reservoir was estimated, considering the existing coverage area, with a capacity of 130 kWp, and expansions of the system to correspond to energy production capacities of 1 MWp, 2.5 MWp and 5 MWp. Different methods were used to estimate the evaporation rates through local meteorological data such as air temperature, humidity, solar radiation, and wind speed, whose results were compared with direct evaporation measurements obtained at the nearest meteorological station. The FAO Penman-Monteith and Linacre method (1977) showed better results for the region. An efficiency of 60.20% in reducing evaporation rates and water-saving by the floating photovoltaic system layout was obtained, which was then used to calculate avoided evaporation volumes, assuming the increases in coverage area and its relationship to energy production capacity, considering the reservoir at full capacity and in the current scenario of water drought. In the second chapter, evaporation rates were estimated for future climate scenarios for the years 2040, 2060, 2080, and 2100 considering the climate change scenarios from the Intergovernmental Panel on Climate Change. PGECLIMA_R software was used to simulate air temperature, humidity, and solar radiation; the wind was obtained through a beta distribution simulation. An increase in evaporation of 31.88% compared to current historical data can be expected towards the end of the century in the worst climate scenario. Therefore, technologies such as the floating photovoltaic system can represent an essential alternative in preventing evaporation today and in the future, becoming a strategic tool in managing water resources.

Keywords: Water Evaporation. Floating Photovoltaic System. Climate Change.

RESUMO

A escassez de água doce é uma grande preocupação devido às mudanças climáticas em algumas regiões do Brasil. As taxas de evaporação da água em reservatórios aumentam com o aumento das temperaturas, o que pode representar um grande desafio para a gestão dos recursos hídricos. A área de cobertura dos sistemas fotovoltaicos flutuantes reduz a quantidade de luz solar na superfície da água, reduzindo as taxas de evaporação da água. Em 2019 foi instalado um sistema fotovoltaico flutuante no reservatório Passaúna, localizado na região metropolitana de Curitiba, Estado do Paraná, sul do Brasil. O objetivo geral deste trabalho é estudar os efeitos do sistema fotovoltaico flutuante sobre a evaporação da água no reservatório do Passaúna. Com base nesse objetivo, o trabalho foi dividido em dois capítulos: no primeiro capítulo foi estimada a evaporação evitada pela instalação do sistema fotovoltaico flutuante no reservatório do Passaúna, considerando a área de cobertura existente, com capacidade de 130 kWp, e um aumento na área de abrangência correspondente a 1 MWp, 2.5 MWp e 5 MWp em capacidade de produção de energia. Diferentes métodos foram utilizados para estimar as taxas de evaporação por meio de dados meteorológicos locais, como temperatura do ar, umidade, radiação solar e velocidade do vento, cujos resultados foram comparados com medições diretas de evaporação obtidas na estação meteorológica mais próxima. O método FAO Penman-Monteith e Linacre (1977) apresentou melhores resultados para a região. Obteve-se uma eficiência de 60,20% na redução das taxas de evaporação e economia de água pelo layout do sistema fotovoltaico flutuante, que foi então utilizado para calcular os volumes de evaporação evitados, assumindo os aumentos de área de cobertura e sua relação com a capacidade de produção de energia, considerando o reservatório em sua capacidade total e no atual cenário de seca hídrica. No segundo capítulo, foram estimadas as taxas de evaporação para cenários climáticos futuros para os anos de 2040, 2060, 2080 e 2100 considerando os cenários de mudanças climáticas do Painel Intergovernamental sobre Mudanças Climáticas. O software PGECLIMA_R foi utilizado para simular a temperatura do ar, umidade e radiação solar; o vento foi obtido através de uma simulação de distribuição beta. Um aumento na evaporação de 31,88% em relação aos dados históricos atuais pode ser esperado para o final do século no pior cenário climático. Portanto, tecnologias como o sistema fotovoltaico flutuante podem representar uma importante alternativa na prevenção da evaporação hoje e no futuro, tornando-se uma ferramenta estratégica na gestão dos recursos hídricos.

Palavras-chave: Evaporação da Água. Sistema Fotovoltaico Flutuante. Mudanças Climáticas.

LIST OF FIGURES

LIST OF TABLES

ABBREVIATIONS

AR	Assessment Report
BDMEP	Meteorological database for Teaching and Research
EPE	Energy Research Office
FAO	Food and Agriculture Organization of the United Nations
FPS	Floating photovoltaic system
GHG	Greenhouse gases
INMET	National Institute of Meteorology
IPCC	Intergovernmental Panel on Climate Change
ISE	Solar Energy Systems
NOAA	National Oceanic and Atmospheric Administration
RCP	Representative Concentration Pathways
Sanepar	Water and Sanitation Company of Paraná State
SSP	Shared Socio-economic Representative Pathways
UEPG	State University of Ponta Grossa
UN-Water	United Nations Water
WMO	World Meteorological Organization

SUMMARY

1 INTRODUCTION

Water is a fundamental component used in the most diverse areas: water is essential in sectors like agriculture and industry besides human consumption.

Water security and shortages are topics of concern due to climate change. Climate change affects, directly and indirectly, water evaporation in reservoirs; it is speculated that, with warmer temperatures, water evaporation would increase considerably, by at least 7.69% in Australia (HARTMANN, 2016; HELFER; LEMCKERT; ZHANG, 2012).

Studies that address innovative and sustainable initiatives for the efficient management of water resources are essential for developing preventive actions against the negative impacts of climate change, such as water scarcity in different parts of the world.

Water losses due to evaporation can represent more than 50% in reservoirs, which can be avoided with efficient management of the water resources. Studies have shown that devices such as floating and suspended covers can reduce the water evaporation rates by up to 90% (TABOADA *et al.*, 2017; YAO, 2010; CRAIG, 2005).

A floating Photovoltaic System (FPS) is a structure supported on a water surface composed of photovoltaic modules, floating and mooring systems, and other equipment such as inverters, transformers, etc. Energy is captured from solar radiation and transformed into electrical energy.

In addition to being a sustainable system that uses renewable energy, FPS can be used to mitigate water supply issues by reducing the evaporation rate of water bodies (LIU *et al.*, 2017; LOPES *et al.*, 2020).

This work is divided into two articles. The first article presents the effects of the Floating Photovoltaic System on water evaporation rates in the Passaúna Reservoir, considering its current coverage area and a possible larger coverage area (1 MWp, 2.5 MWp and 5 MWp) from a future expansion of the system. Meteorological data such as air temperature, humidity, wind speed and solar radiation were used to estimate the evaporation rates through different methods.

The second article shows how climate changes can affect the water evaporation rates in reservoirs. PGECLIMA_R software was used to simulate climate scenarios of evaporation water losses in the Passaúna Reservoir, based on the Sixth

Assessment Report of the United Nations Intergovernmental Panel on Climate Change – IPCC AR6, using meteorological data from the Meteorological database for Teaching and Research (BDMEP) of the National Institute of Meteorology (INMET).

The preliminary results presented in both articles will be helpful as a reference for future studies. FPS represents a viable and sustainable solution for saving water in reservoirs, especially in periods of water scarcity that are becoming more evident nowadays due to climate changes.

2 OBJECTIVES

2.1 GENERAL OBJECTIVE

The main objective of this work is to study the effects of the floating photovoltaic system on the water evaporation rates in the Passaúna reservoir.

2.2 SPECIFIC OBJECTIVES

Analyze the daily and annual average of the water evaporation rates in the Passaúna Reservoir using local meteorological data;

Evaluate the influence of the current area and a possible larger area of the floating photovoltaic system covering the water surface on the water evaporation rates in the Passaúna Reservoir;

Simulate future climate change scenarios and their effects on the water evaporation rate in the Passaúna Reservoir.

3 LITERATURE REVIEW

3.1 WATER SCARCITY

Water scarcity is one of the aspects of great relevance on the world stage. With the growing demand for this resource - used in the most diverse purposes, from the primary to the tertiary sector - its efficient use is crucial for human life and the economy.

According to the Food and Agriculture Organization of the United Nations and United Nations Water (FAO; UN-Water, 2021), water is essential for life; therefore, the need to reduce its use, ensure access and minimize water stress is required. Sustainable, inclusive, and integrated management of water resources must be promoted globally. About 3.6 billion people face inadequate access to water, at least one month a year, considering water as a priority for adaptation for the sustainable use of resources (WORLD METEOROLOGICAL ORGANIZATION – WMO, 2021).

According to Neves (2015), the growing world demand for water is crucial in encouraging studies to manage this resource. The same author also explains that water availability is estimated by the inputs and outputs of the water balance, with the main input being the rainfall and the output being the evapotranspiration.

Alternatives to optimize water resources are increasingly necessary with the growing environmental concern and the need for the rational use of water. Craig (2005) estimates that half of the reservoir water is lost through evaporation.

Water reservoirs are fundamental in developing water resources management policies, as well as a way to control variations in water availability in periods of drought and floods. Water evaporation represents an essential value for the control of outputs and is a way of monitoring the amount of water resources available in reservoirs (WURBS; AYALA, 2013).

According to Pereira (2004), there are two problems in managing water resources - the inconsistency in the flows calculated by historical series; and evaporative losses in reservoirs. Reliable estimates are essential for water resources planning and management.

3.2 EVAPOTRANSPIRATION AND EVAPORATION

Evapotranspiration is the combined process of evaporation and transpiration. Evaporation is when the water is converted into vapor, and transpiration is the vaporization of water contained in plant tissues (ALLEN *et al.*, 1998). The same authors added, "Evaporation and transpiration occur simultaneously and there is no easy way to distinguish the two processes" (p. 3).

Empirical evapotranspiration equations have been used to estimate water evaporation from lakes and reservoirs (PEREIRA, 2004; CRAIG, 2005b; HELFER; LEMCKERT; ZHANG, 2012; MCMAHON *et al.*, 2013; KOHLI; FRENKEN, 2015; HASSAN *et al.*, 2015; VIEIRA, *et al.*, 2016; TABOADA *et al.*, 2017; COELHO *et al.*, 2018; BONTEMPO SCAVO *et al.*, 2020; HAAS *et al.*, 2020; RODRIGUES; RAMALHO; MEDEIROS, 2020).

Evaporation is a phenomenon that occurs due to the incidence of solar energy on the Earth. By absorbing heat, water accumulates energy in its molecules and eventually evaporates - particularly in the hottest periods and areas of the globe. This rate depends on factors such as surface area, air humidity, wind speed, temperature, and atmospheric pressure (OLIVEIRA, 2009).

Neves (2015) describes evaporation as a difficult measure to obtain; therefore, it is estimated by equations as a function of climatological variables, using data from meteorological stations.

According to Hartmann (2016), evaporation from a reservoir is limited by the surface water supply, the energy available to achieve the latent heat of vaporization, and the ability of the surface air to accommodate the water vapor. Potential evaporation from reservoirs can be used to understand how the hydrological water cycle is affected by the global mean air temperature change so that potential evaporation will increase in warmer climates.

Studies to estimate reservoir evaporation date back to the beginning of the 20th century. It is quantified by a variety of meteorological data, such as incidence of solar radiation, wind speed, relative humidity, air temperature, and atmospheric pressure. In addition, it is a complex variable to obtain directly, so methods for indirect estimation were developed (HARWELL, 2012; CURTARELLI *et al.*, 2013).

Likewise, Hassan *et al.* (2015) state that when considering the security of the water availability - especially in arid regions; the reduction of the water evaporation in

reservoirs is essential. According to the authors, it is possible to relate evaporation reduction with the surface areas covered in reservoirs.

Evaporation loss is a challenge in reservoir efficiency, with a focus on arid regions and areas with water scarcity – in that way, FPS would be a solution for the evaporation mitigation in reservoirs (AMINZADEH; LEHMANN; OR, 2018).

3.3 EVAPORATION UNDER CLIMATE CHANGE SCENARIOS

IPCC is the Intergovernmental Panel on Climate Change and has provided scientific knowledge on global climate change. According to the Synthesis Report from the Fifth Assessment Report of the IPCC (2014), the world has undoubtedly presented, especially since the 1950s, an increase in the temperatures due to greenhouse gas emissions, as shown in Figure 1.

Figure 1 – Globally mean combined land and ocean surface temperature anomaly (a) and globally mean concentrations of greenhouse gases (b).

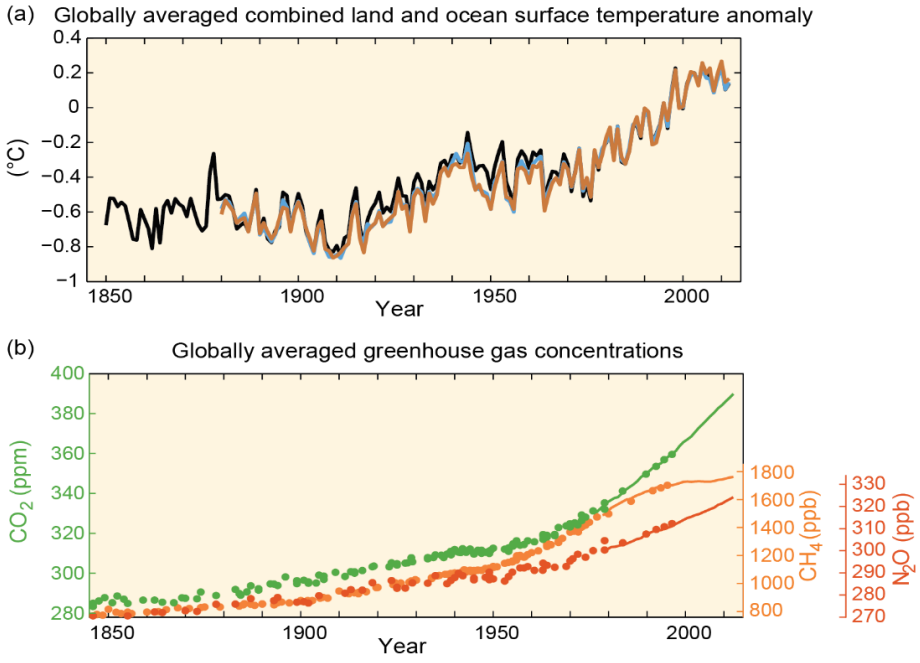

Note: (a) Globally averaged combined land and ocean surface temperature anomalies relative to the average over the period of 1986 to 2005. (b) Atmospheric concentrations of carbon dioxide (CO_2), methane (CH_4), and nitrous oxide (N_2O).
Source: Adapted from the Synthesis Report of the Fifth Assessment Report (IPCC, 2014).

According to the National Centers for Environmental Information (NOAA, 2022), 2020 was the second warmest year in the last 141 years, with an average

temperature increase of +0.98ºC. The seven warmest years in the period 1880-2020 have been recorded since 2014 (Fig.2).

Figure 2 – Global Land and Ocean temperature anomalies.

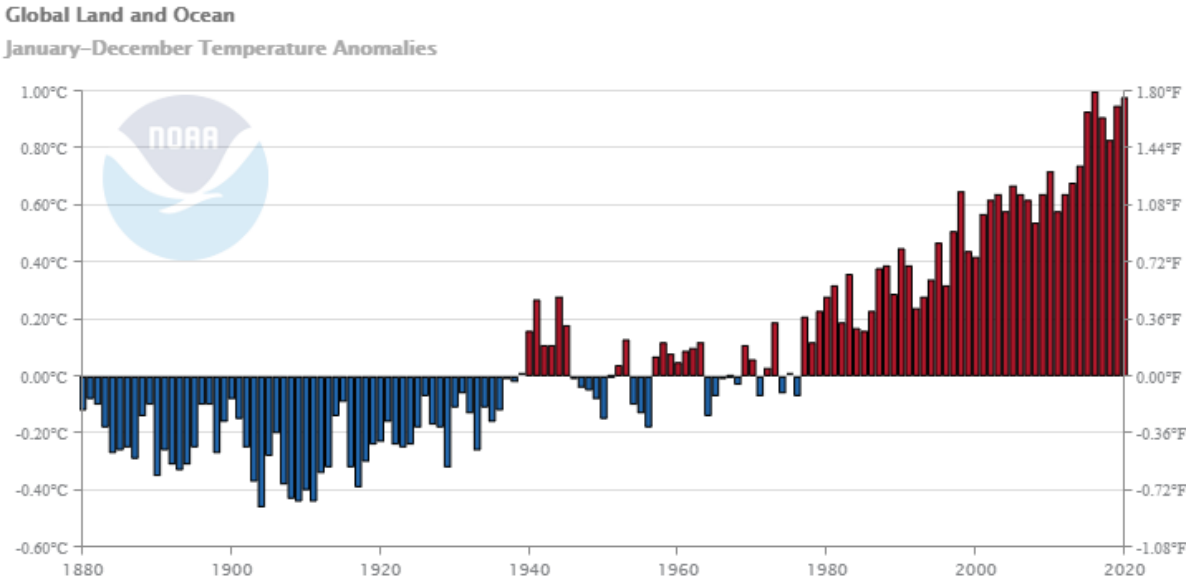

Source: National Centers for Environmental Information (NOAA, 2022).

The scenarios in the Sixth Assessment Report of the IPCC (2021), called SSPs – Shared Socio-economic Representative Pathways, are based on the possible future socioeconomic development of the anthropogenic drivers of climate change. Scenarios are labelled as “SSPx-y”, where the “y” refers to the approximate level of radiative forcing (W m-²), and the “SPPx” refers to the socioeconomic trend (IPCC, 2021). The scenarios include low greenhouse gases (GHG) emissions (SPP1-1.9) to very high GHG emissions (SPP5-8.5) by the end of the century 2100. According to the IPCC (2021), the SSPs were developed to complement the Representative Concentration Pathways (RCPs) scenarios of the Fifth Assessment Report.

Therefore, scenarios from both extremes can be used to simulate future climate change, designating one as optimistic and the other as pessimistic. In the long term, an optimistic scenario would lead to an increase in the variation of the global mean surface temperature change in a probable range of 1.0ºC to 1.8ºC in 2100. The pessimistic scenario would increase from 3.3ºC to 5.7ºC in the same period, as shown in Table 1 (IPCC, 2021).

Table 1 – Changes in global surface temperature relative to the average global surface temperature of the period of 1850-1990.

Scenario	Near term, 2021-2040		Mid-term, 2041-2060		Long term, 2081-2100	
	Best estimate (ºC)	Very likely range (ºC)	Best estimate (ºC)	Very likely range (ºC)	Best estimate (ºC)	Very likely range (ºC)
SSP1-1.9	1.5	1.2 to 1.7	1.6	1.2 to 2.0	1.4	1.0 to 1.8
SSP1-2.6	1.5	1.2 to 1.8	1.7	1.3 to 2.2	1.8	1.3 to 2.4
SSP2-4.5	1.5	1.2 to 1.8	2.0	1.6 to 2.5	2.7	2.1 to 3.5
SSP3-7.0	1.5	1.2 to 1.8	2.1	1.7 to 2.6	3.6	2.8 to 4.6
SSP5-8.5	1.6	1.3 to 1.9	2.4	1.9 to 3.0	4.4	3.3 to 5.7

Source: Adapted from the Sixth Assessment Report (IPCC, 2021).

O'neill *et al.* (2017) describe the SPP narratives, in which the SPP1 or optimistic scenario would lead to a sustainable development path, with greater environmental awareness and gradual change in lifestyles, while the SPP5 or pessimistic scenario would be a development fueled by fossil fuels, with dependence on fossil fuels and lack of environmental concern. Based on AR-5 (IPCC, 2014), it is possible to assume that an optimistic scenario would include rigorous mitigation of GHG emissions reduction, as the pessimistic scenario would not make efforts in this direction.

Climate change would increase the risk related to water scarcity and droughts. Consequently, with increasing global temperature, the water bodies' evaporation rate would also increase (IPCC, 2014).

According to climate simulations in a reservoir in Australia, Helfer; Lemckert; Zhang (2012) showed a significant increase in evaporation rates from 2030 to 2050 and 2070 to 2090, being 5.6% and 14.5%, respectively, above the rates represented by the current climate scenario.

Through simulations with the RCPs scenarios of the IPCC, Bazzi *et al.* (2020) presented the predictions of the variation of evaporation losses for the period 2030-2050 and 2080-2100. Expected evaporation is likely to increase in any simulated scenarios. The increase in cloud cover and air humidity would possibly have a negative effect on the intensity of evaporation.

Climate change affects not only the air temperature but also other parameters such as cloudiness and air humidity, influencing water evaporation rates. The importance of this topic is demonstrated where an appropriate knowledge of evaporation behavior would lead to assertive water management.

Water resources have been threatened by climate change. Bazzi *et al.* (2020) indicated an overall increase in the rate of evaporation under climate change of more than 300 mm in the period 2080-2100, in the Chahnimeh Reservoirs of the Sistan Plain, in Iran.

The Penman evaporation method has shown the most realistic estimates for the temporal dynamics of evaporation, using as input data four variables: net radiation (Rn), wind speed (u), air temperature (Ta), and relative humidity (Rh) (DONOHUE; MCVICAR; RODERICK, 2010; LIU; MCVICAR, 2012). A decreasing trend of Rn and u may compensate for the increased evaporation by high Ta, indicating the complex interaction among meteorological parameters (LIU; MCVICAR, 2012). Although climate change predicts an increase in the air temperature, it is not possible to state that this will induce an increase in water evaporation as different variables affect the water evaporation (DONOHUE; MCVICAR; RODERICK, 2010).

Bai *et al.* (2020) corroborate with the study of the authors above-cited, confirming that the decrease in the net radiation and wind speed contribute to the reduction of water evaporation. The study correlated the atmospheric evaporation demand to the actual evaporation, showing that a trend toward higher temperatures would not compensate for decreases in the atmospheric evaporation demand resulted by the Rn.

Meteorological simulators such as PGECLIMA_R are designed to predict a synthetic series of weather data that correlates with historical series. The performance of PGECLIMA_R software has been studied and showed a high correlation between predicted and observed weather data (VIRGENS FILHO *et al.*, 2014).

Climate change simulations can be used to observe different things. The PGECLIMA_R software can also be used to predict changes in the four driven evaporation variables under IPCC climate change scenarios.

PGECLIMA_R has already been used in other master's works: to predict solar radiation and estimate the potential of the photovoltaic generation under climate change scenarios (SGARBOSSA, 2019); simulate precipitation levels and predict impacts on rainwater storages (COSTA, 2016); contemplate rainwater harvesting combined with photovoltaic energy under climate change scenarios (TSUNETO; VIRGENS FILHO, 2020).

3.4 METHODS TO ESTIMATE EVAPORATION FROM OPEN WATER

3.4.1 Linacre Equation

Linacre (1977) proposed a methodology that uses only latitude, elevation, and temperature data to estimate evaporation rates, which can be applied in cases where there is not enough data to use other methods. Based on Penman (1948), a simplified equation to estimate the evaporation in lakes (eq.1) was proposed:

$$E=\frac{\frac{700(Ta+0.006h)}{100-\phi}+15(Ta-Td)}{(80-Ta)} \quad (1)$$

Where:

E = estimated evaporation $(mm\ day^{-1})$

Ta = mean air temperature (ºC)

Td = mean dew-point (ºC)

ϕ = latitude (degrees)

h = elevation (m)

Td (ºC) is the mean dew-point and can be obtained using the Tetens equation, where the saturation vapor pressure and air vapor pressure values are needed (TETENS, 1930; apud ALLEN *et al.*, 1998).

The saturation vapor pressure and vapor pressure are obtained as follows (eq. 2 and 3) (DLOUHÁ; DUBOVSKÝ; POSPÍŠIL, 2021):

$$e_s = 0.611*\exp\left(\frac{17.27*T}{T+237.3}\right) \quad (2)$$

$$e_a = \left(\frac{e_s*RH}{100}\right) \quad (3)$$

Where:

e_s = saturation vapor pressure (kPa)

e_a = vapor pressure (kPa)

RH = relative humidity (%)

T = mean air temperature (ºC)

exp = Euler's number

Carvalho *et al.* (2010) defined the dew-point temperature as the point where a portion of air can be cooled down, where constant values of vapor pressure and water vapor will occur in saturation; thus, there will be a temperature value where the saturation vapor pressure will be equal to the vapor pressure.

With the saturation vapor pressure and the vapor pressure is possible to obtain the dew-point temperature using the Tetens equation (eq. 4) (1930; apud CARVALHO *et al.*, 2010):

$$Td = \frac{237.3Log(\frac{e_a}{0.6108})}{7.5\text{-}Log(\frac{e_a}{0.6108})} \quad (4)$$

Where:

Td = mean dew-point temperature (ºC)

e_a = vapor pressure (kPa)

Linacre (1993) proposed a new equation for estimating monthly mean evaporation from lakes as follows:

$$E_0 = (0.015+0.0042T+10^{-6}z)[0.8R_s-40+2.5F*u(T-Td)] \quad (5)$$

Where:

E_0 = estimated evaporation $(mm\ day^{-1})$

T = daily mean air temperature (ºC)

Td = mean dew-point temperature (ºC)

$F = 1.0-8.7*10^{-5}z$ - where z is the elevation (m)

R_s = solar irradiance $(W\ m^{-2})$

u = wind speed $(m\ s^{-1})$

Although both Linacre's equations are similar, the most recent equation (LINACRE, 1993) also includes wind speed and solar radiation in the estimative, approximating the directly measured evaporation more accurately, giving estimates within about 0.25 mm day^{-1}.

3.4.2 Rohwer

The water losses by evaporation in reservoirs motivated the study of Rohwer (1931), a method based on aerodynamics was proposed, as shown in (eq. 6):

$$E = (0.44+0.118*W)(e_s-e_d) \quad (6)$$

Where:

E = estimated evaporation (in day^{-1})

W = wind speed (mph)

e_s = saturation vapor pressure (inHg)

e_d = saturation vapor pressure at dew-point temperature (inHg)

Since Rohwer's method gives evaporation in inches per day, it can be converted to mm per day by multiplying the result by 25.4. The saturation vapor pressure at the dew point temperature can be obtained by substituting the temperature in the Tetens equation (eq. 2) for the dew-point temperature.

3.4.3 Valiantzas

According to Valiantzas (2006), evaporation is one of the main components of the hydrologic cycle, and its estimation use is of great importance in water resources management. A simplified method to estimate the evaporation based on the Penman equation (1948) was also proposed by Valiantzas (2006), according to (eq. 7):

$$E_{pen} \approx 0.051(1-\alpha)R_s\sqrt{T+9.5}-0.188*(T+13)\left(\frac{R_s}{R_a}-0.194\right)* \left(1-0.00014(0.7T_{max}+0.3T_{min}+46)^2\sqrt{\frac{RH}{100}}\right) +0.049(T_{max}+16.3)\left(1-\frac{RH}{100}\right)(a_u+0.536u) \quad (7)$$

Where:

E_{pen} = estimated evaporation $\left(mm\ day^{-1}\right)$

R_s = incoming solar radiation $\left(MJ\ m^{-2}\ day^{-1}\right)$

α = water albedo

T = mean air temperature (ºC)

T_{max}= maximum air temperature (ºC)

T_{min}= minimum air temperature (ºC)

R_a= extraterrestrial radiation $\left(MJ\ m^{-2}\ day^{-1}\right)$

a_u = wind function constant

RH = relative humidity (%)

u = wind speed $\left(m\ s^{-1}\right)$

Meteorological data to estimate evaporation are widely used, as direct measurement techniques imply time-consuming procedures and expensive equipment (VALIANTZAS, 2006).

3.4.4 Penman-Monteith Equation

Hartmann (2016) presents the Penman equation (1948) as one of the methods to estimate the potential daily evaporation. This method was later standardized by the FAO (Food and Agriculture Organization of the United Nations) - known as Penman-Monteith, the combination of the Penman (1948) and Monteith (1965) methods. Other authors recommend using the Penman-Monteith equation as one of the closest in comparison to direct measurement by evaporimeters (HELFER;

LEMCKERT; ZHANG, 2012; TABOADA *et al.*, 2017; BONTEMPO SCAVO *et al.*, 2020).

Allen *et al.* (1998) used the Penman-Monteith equation (1965) and provided a new combined equation from the original to estimate the evaporation, including aerodynamic and surface resistance.

Based on mathematical modelling, Bontempo Scavo *et al.* (2020) proposed polynomial equations that are less complex than the original Penman-Monteith method, which is indicated in situations where there is not enough data from weather stations to apply the Penman-Monteith method. The authors added that values estimated by the Penman-Monteith method are correlated with those measured by evaporimeters.

The FAO Penman-Monteith equation takes into account the evapotranspiration of the reference crop; however, Kohli; Frenken (2015) stipulate that for open water, the crop coefficient would be equal to 1, and there would be no occurrence of transpiration in the element, thus, leading to the water evaporation being equal to the reference evapotranspiration, as follows:

$$ET_o = E \tag{8}$$

Where:

E = estimated evaporation $\left(mm\ day^{-1}\right)$

ET_o = reference crop evapotranspiration $\left(mm\ day^{-1}\right)$

FAO Penman-Monteith requires weather data such as air temperature, humidity, solar radiation, and wind speed. It also requires data from the study area, such as altitude above sea level and latitude (ALLEN *et al.*, 1998).

Equation (9) represents the FAO Penman-Monteith (ALLEN *et al.*, 1998):

$$E = \frac{0.408\Delta(R_n\text{-}G) + \gamma\left(\frac{900}{T+273}\right)u_2(e_s\text{-}e_a)}{\Delta+\gamma(1+0.34u_2)} \tag{9}$$

Where:

E = estimated evaporation $\left(mm\ day^{-1}\right)$

R_n = net radiation $(MJ\ m^{-2}day^{-1})$

G = soil heat flux density $(MJ\ m^{-2}day^{-1})$

T = mean air temperature (ºC)

u_2 = wind speed at 2 m height $(m\ s^{-1})$

e_s = saturation vapor pressure (kPa)

e_a = vapor pressure (kPa)

Δ = slope vapor pressure curve $(kPa\ ºC^{-1})$

γ = psychrometric constant $(kPa\ ºC^{-1})$

Soil heat flux density (G) can be ignored for daily calculation due to its low value and does not interfere with the final evaporation result (ROCHA *et al.*, 2011; ALLEN *et al.*, 1998).

Saturation vapor pressure and vapor pressure are obtained using the equations (2) and (3) shown earlier.

When not provided by weather station data, the atmospheric pressure (P) is obtained from the elevation of the study area (eq. 10).

$$P = 101.3\left(\frac{293-0.0065z}{293}\right)^{5.26} \quad (10)$$

Where:

P = atmospheric pressure (kPa)

z = elevation above sea level (m)

According to Allen *et al.* (1998), the latent heat of vaporization (λ) "varies slightly" (p. 31) and the value of 2.45 MJ kg^{-1} can be assumed. It can be also calculated using the equation (11) given by Bueno (2014):

$$\lambda = 2.501-(2.361*10^{-3})*Ta \quad (11)$$

Where:

λ = latent heat of vaporization $(MJ\ kg^{-1})$

Ta = mean air temperature (ºC)

The psychometric constant can be determinate by the equation 12 (ALLEN *et al.*, 1998):

$$\gamma = \frac{C_p P}{\varepsilon \lambda} \quad (12)$$

Where:

γ = psychrometric constant $\left(kPa\ ºC^{-1}\right)$

P = atmospheric pressure (kPa)

λ = latent heat of vaporization $\left(MJ\ kg^{-1}\right)$

C_p = specific heat at constant pressure, $1.013*10^{-3}$ $\left(MJ\ kg^{-1}\ ºC^{-1}\right)$

ε = ratio molecular weight of water vapor/dry air, 0.622

Simplifying the equation (12), it is possible to obtain the psychrometric constant by the equation (13):

$$\gamma = 0.665*10^{-3}P \quad (13)$$

The method recommends using the saturation vapor pressure values obtained from equation (2) using the maximum and minimum air temperature (DLOUHÁ; DUBOVSKÝ; POSPÍŠIL, 2021). Using the mean air temperature would result in lower estimates of the saturation vapor pressure (eq. 14).

$$e_s = \frac{e_{s(max)} + e_{s(min)}}{2} \quad (14)$$

The FAO Penman-Monteith method describes the slope of the saturation vapor pressure curve as “the relationship between saturation vapor pressure and temperature” (ALLEN *et al.*, p. 37, 1998). Thus, the equation (15) is given:

$$\Delta = \frac{4098(0.6108\exp\left(\frac{17.27T}{T+237.3}\right)}{(T+237.3)^2} \quad (15)$$

The same equation can be represented by (eq. 16):

$$\Delta = \frac{4098e_s}{(T+237.3)^2} \quad (16)$$

Where:

Δ = slope of saturation vapor pressure curve at air temperature (kPa $^oC^{-1}$)

e_s = saturation vapor pressure (kPa)

T = air temperature (^oC)

exp = Euler's number

Solar radiation that penetrates the atmosphere can be absorbed, reflected or scattered by the environment. The net radiation is the difference between the input and output energy reaching a surface (FLUMIGNAN *et al.*, 2018).

Bueno (2014) highlights that solar radiation directly impacts the rate of water evaporation. More radiation is received, more available energy; thus, the rate of evaporation increases.

Data obtained from weather stations can be described as incident solar radiation (R_s), which is the amount of radiation that reaches a horizontal plane. Therefore, net radiation can be derived from this data.

There is a need for other parameters such as extraterrestrial radiation (R_a) to calculate the net radiation (R_n). Extraterrestrial radiation is the horizontal radiation at the top of the Earth's atmosphere. This phenomenon contemplates the angle of the sun's rays and its change during the year for which area, considering the latitude, as described in equation (17) (ALLEN *et al.*, 1998).

$$Ra = \frac{24(60)}{\pi} G_{sc} d_r [\sin(\varphi)\sin(\delta) + \cos(\varphi)\cos(\delta)\sin(\omega_s)] \quad (17)$$

Where:

R_a = extraterrestrial radiation $\left(MJ\ m^{-2}\ day^{-1}\right)$

G_{sc} = solar constant, 0.0820 $\left(MJ\ m^{-2}\ min^{-1}\right)$

d_r = inverse relative distance Earth-Sun (radians)

ω_s = sunset hour angle (radians)

φ = latitude (radians)

δ = solar declination (radians)

Equations (18), (19), and (20) are used to obtain the inverse relative distance Earth-Sun, solar declination and the sunset angle, respectively (ALLEN *et al.*, 1998).

$$d_r=1+0.033\cos\left(\frac{2\pi}{365}J\right) \quad (18)$$

$$\delta=0.409\sin\left(\frac{2\pi}{365}J-1.39\right) \quad (19)$$

$$\omega_s=\arccos\left[-\tan(\varphi)\tan(\delta)\right] \quad (20)$$

Where:

d_r = inverse relative distance Earth-Sun (radians)

δ = solar declination (radians)

ω_s = sunset hour angle (radians)

J = number of the day in the year

The shortwave radiation is calculated by the equation (21), where the water albedo is considered (ALLEN *et al.*, 1998).

$$R_{ns} = (1-\alpha)R_s \quad (21)$$

Where:

R_{ns} = shortwave radiation $\left(MJ\ m^{-2}\ day^{-1}\right)$

α = albedo or reflection coefficient

R_s = incoming solar radiation $\left(MJ\ m^{-2}\ day^{-1}\right)$

According to Allen *et al.* (1998), clear-sky solar radiation can be obtained by the equation (22).

$$R_{so} = \left(0.75+2*10^{-5}z\right)R_a \quad (22)$$

Where:

R_a = extraterrestrial radiation $\left(MJ\ m^{-2}\ day^{-1}\right)$

R_{so} = clear-sky radiation $\left(MJ\ m^{-2}\ day^{-1}\right)$

z = elevation above sea level (m)

Water vapor, clouds, carbon dioxide, and dust affect the radiation, which is absorbed, reflected, and diffused in the atmosphere. The outgoing longwave net radiation considers this effect reported in the Stefan-Boltzmann law, which can be obtained by the equation (23) (ALLEN *et al.*, 1998).

$$R_{nl} = \sigma\left(\frac{T_{max,k}^{\ 4}+T_{min,k}^{\ 4}}{2}\right)\left(0.34-0.14\sqrt{e_a}\right)\left(1.35\frac{R_s}{R_{so}}-0.35\right) \quad (23)$$

Where:

R_{nl} = net outgoing longwave radiation $\left(MJ\ m^{-2}\ day^{-1}\right)$

σ = Stefan-Boltzmann Constant $\left(MJ\ m^{-2}\ day^{-1}\right)$

$T_{max,k}$ = maximum day temperature (K=ºC+273.16)

$T_{min,k}$ = maximum day temperature (K=ºC+273.16)

e_a = vapor pressure (kPa)

R_s = measured solar radiation $\left(MJ\ m^{-2}\ day^{-1}\right)$

R_{so} = clear-sky radiation $\left(MJ\ m^{-2}\ day^{-1}\right)$

By considering the above-mentioned equations, it is possible to obtain the final net radiation which represents the difference between the incoming shortwave net radiation and the outgoing longwave net radiation (eq. 24).

$$R_n = R_{ns} - R_{nl} \quad (24)$$

Where:

R_n = net radiation $\left(MJ\ m^{-2}\ day^{-1}\right)$

R_{nl} = net outgoing longwave radiation $\left(MJ\ m^{-2}\ day^{-1}\right)$

R_{ns} = net incoming shortwave radiation $\left(MJ\ m^{-2}\ day^{-1}\right)$

The wind speed function is described in the FAO method and must be used to adjust data obtained at heights other than the standard 2 m (eq. 25) (ALLEN *et al.*, 1998).

$$u_2 = u_z \frac{4.87}{\ln(67.8z - 5.42)} \quad (25)$$

Where:

u_2 = wind speed at 2m $\left(m\ s^{-1}\right)$

u_z = measure wind speed at z m $\left(m\ s^{-1}\right)$

z = height of measurement (m)

After obtaining the values from the equations (2), (3), (12), (14), (24), and (25) described above, the results can be applied to equation (9) resulting in the evaporation in mm/day.

3.4.5 Hargraves-Samani Equation

Regarding the difficulty of available climatological data, Hargraves-Samani developed the equation (26) where the required data is only the maximum and minimum air temperature, resulting in a reasonable accuracy compared to the lysimeter data and the Penman equation (HARGRAVES; SAMANI, 1985).

$$ETP = 0.0023 R_a (T_{max} - T_{min})^{0.5} (T_{mean} + 17.8) \quad (26)$$

Where:

ETP = potential evapotranspiration $\left(mm\ day^{-1}\right)$

T_{mean} = mean air temperature (ºC)

T_{max} = maximum air temperature (ºC)

T_{min} = minimum air temperature (ºC)

R_a = extraterrestrial radiation $\left(MJ\ m^{-2}\ day^{-1}\right)$

As explained earlier, empirical equations of evapotranspiration have been used to estimate water evaporation from lakes and reservoirs.

Although the Hargraves-Samani method considers evaporation and transpiration from the vegetation, resulting in potential evapotranspiration, it can be compared to the Linacre and Penman-Monteith methods. The difference between them is that in the Penman-Monteith equation, the water albedo is considered instead of the grass albedo, and in the Linacre equation, only the air temperature and altitude are considered.

3.4.6 Area Coverage Efficiency

According to Assouline; Narkis; Or (2011), there is no evidence that the reduction in water evaporation is proportional to the covered area by a floating cover. The authors studied the relationships between water evaporation and surface coverage with different types of openings in the covered surface. The evaporation fraction of the surface area covered is described by equation (27) (ASSOULINE; NARKIS; OR, 2011).

$$\alpha = \frac{S_c}{S},\ 0 \leq \alpha \leq 1 \qquad (27)$$

Where:

α = evaporating fraction

S_c = evaporating area of a partially covered surface

S = considered area of water surface

Equation (28) represents the covered fraction of this surface area:

$$\chi = 1-\alpha, \quad 1 \leq \chi \leq 0 \tag{28}$$

Assouline; Narkis; Or (2010) also studied the relative water evaporation between a covered and uncovered water surface with distributed openings in the covered surface, described in equation (25), and the relative evaporation of water for large openings in the covered surface described in equation (26):

$$\frac{E_c}{E} = \alpha^{1/2} \tag{29}$$

$$\frac{E_c}{E} = \alpha^{2/3} \tag{30}$$

Where:

α = evaporating fraction

E_c = evaporation rate for the covered system

E = evaporation rate for the uncovered system

The evaporation reduction efficiency of partial covers can be defined as (ASSOULINE; NARKIS; OR, 2011):

$$\varepsilon = 1-\frac{E_c}{E} \tag{31}$$

Thus, equations (23), (24), (25), (26) and (27) can lead to the relationship between the evaporation reduction efficiency (ε) and the covered fraction of the surface area (χ) (ASSOULINE; NARKIS; OR, 2011):

$$\varepsilon = 1-(1-\chi)^{1/2} \text{ – for small distributed openings} \tag{32}$$

Where:

ε = evaporation reduction efficiency for small distributed openings

$$\varepsilon = 1-(1-\chi)^{2/3} \text{ – for large individual openings} \quad (33)$$

Where:

ε = evaporation reduction efficiency for large individual openings

3.5 FLOATING PHOTOVOLTAIC SYSTEMS

Different technologies can be applied to reduce evaporation in lakes and reservoirs, such as suspended covers or floating systems. Suspended covers can be described as horizontal structures over water surfaces that need cables or poles for their structure and the floating systems are supported directly on water surfaces using some form of anchoring mechanism to fix them (YAO *et al.*, 2010).

Floating systems can be exemplified as devices made of floating material, whereas suspended systems can be membranes that guarantee a protective barrier to reduce evaporation.

The efficiency of evaporation reductions in those technologies is related to the reduction of solar radiation, containment of water vapor, and reduction of wind speeds at the water surface (CRAIG *et al.*, 2005; YAO *et al.*, 2010).

Floating photovoltaic systems are installed on the water surface in lakes, reservoirs and ponds, with a floating platform where the photovoltaic modules are supported. Therefore, the FPS covers the water surface, reducing evaporation rates without the need for land works or structural foundations. In addition, they represent a renewable energy source with great potential for electric energy production (TABOADA *et al.*, 2017; MAUÉS, 2019; BONTEMPO SCAVO *et al.*, 2020).

The largest floating photovoltaic plants are located in Asia. In Guqiao, China, a floating photovoltaic plant with a capacity of 150 MWp was installed, totalling 645,000 photovoltaic modules. Another 88,038.76 kWp floating photovoltaic plant is located in Changhua, Taiwan, having 279,488 photovoltaic modules and occupying an area of 86.16 ha (SUNGROW, 2021; CIEL & TERRE INTERNATIONAL, 2021). Both are shown in Figure 3.

Figure 3 – Floating photovoltaic plants in Asia

(a) **(b)**

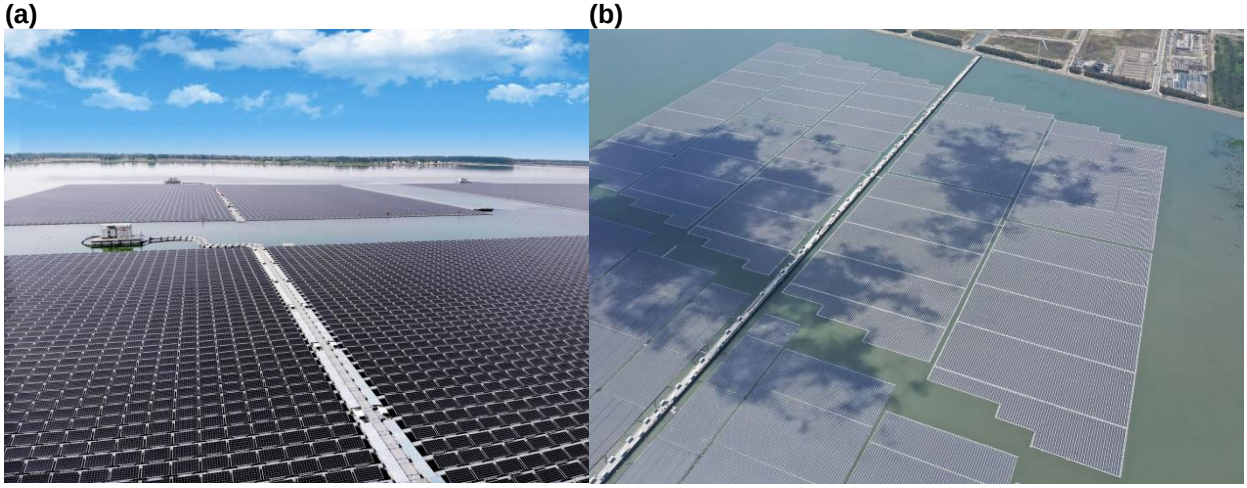

Note: (a) Guqiao floating photovoltaic plant; (b) Changhua floating photovoltaic plant
Source: Sungrow, 2021; Ciel & Terre International, 2021.

Bontempo Scavo *et al.* (2020) studied different types of structures used to support the photovoltaic modules installed on the water - floating and suspended systems (Fig.4). Based on the results of this study photovoltaic modules with full coverage presented the best performance (Figure 4A). The suspended system covering 30% of the reservoir area showed an evaporation reduction of 18% (Fig. 4B and C); 49% for floating systems with full coverage below the photovoltaic modules (Fig. 4A); and 42% for flexible photovoltaic modules in direct contact with the water (Fig. 4D). They concluded that the floating photovoltaic modules of type (A) - in Figure 4 obtained the most efficiency in the evaporation reduction.

Figure 4 – Typologies of photovoltaic modules, (A) module with covered surface below, (B) modules without covering below, (C) suspended system, (D) flexible modules.

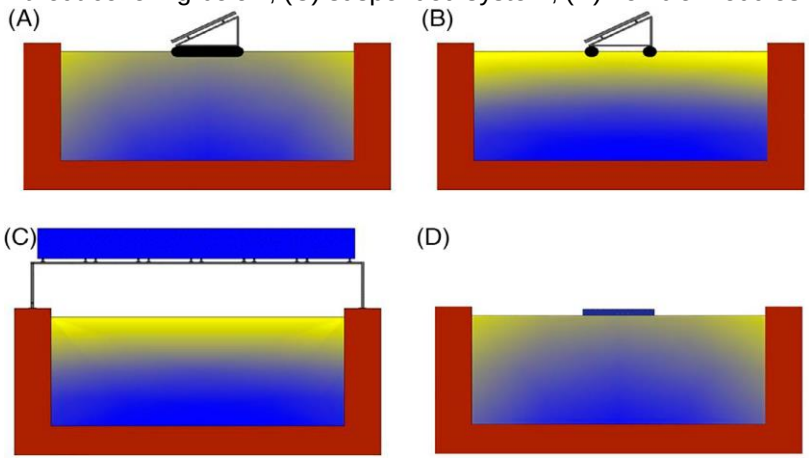

Source: Bontempo Scavo *et al.*, (2020).

The modular floating devices used in the FPS installed in the Passaúna Reservoir can be easily removed or added, ensuring the system's expansion (Figure 5). This modular floating device supports the photovoltaic modules with dimensions of 1960 mm x 991 mm x 40 mm and maximum rated power of 330W each.

Figure 5 – Floating Devices used in the FPS of Passaúna Reservoir

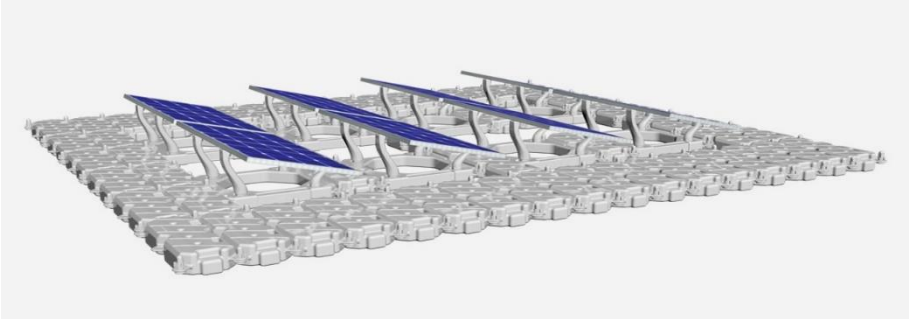

Source: Xiamen Mibet Energy Co. Ltd. (2021).

Floating photovoltaic systems can also present a better efficiency gain than ground-mounted photovoltaic systems; a study carried out in the Brazilian semiarid region observed an efficiency gain ranging from 9.52% to 14.5% (SACRAMENTO *et al.*, 2015). The authors also indicated that an FPS covering 5% of the studied reservoir area could supply 7.4% to 18.8% of the total electricity demand.

3.6 PHOTOVOLTAIC ENERGY IN BRAZIL

According to the Brazilian Electricity Regulatory Agency – ANEEL (2022), Brazil had an equivalent power production of 182,799,497.74 kW, the most significant production being from hydroelectric plants. Despite being a country favored by solar incidence, only 2.67% of the total energy production is provided by solar photovoltaic energy.

Although little explored, photovoltaic energy presents significant growth in Brazil, as stated in the National Energy Balance Report from EPE – Energy Research Office (2020). From 2018 to 2019, there was a 92.2% increase in photovoltaic solar energy generation, from 3.461 GWh to 6.655 GWh.

According to the Brazilian Solar Energy Atlas, photovoltaic energy production in Brazil has great potential. As a comparison, the less sunny area in Brazil would

have better productivity than the sunniest area in Germany (PEREIRA *et al.*, 2017). Regardless of having a growth trend in using photovoltaic energy, Brazil lags far behind Germany. According to the Fraunhofer Institute for Solar Energy Systems - ISE (2021), Germany had a production of 51,420 GWh by photovoltaic energy in 2020, corresponding to 10.5% of the country's energy matrix; however, an increase of 9.3% compared to the previous year (BURGER, 2020).

Figure 6 represents the map of total daily global horizontal irradiation in Brazil, with an average of 3,500-6,250 Wh/m².day. Figure 7 represents the map of daily global horizontal irradiation in Germany, with an average of 2,600-3,400 Wh/m².day.

As seen in Figures 6 and 7, although Brazil has higher solar irradiation, photovoltaic energy generation is low compared to Germany, which has relatively low solar incidence.

Figure 6 – Solar Photovoltaic Generation Potential.

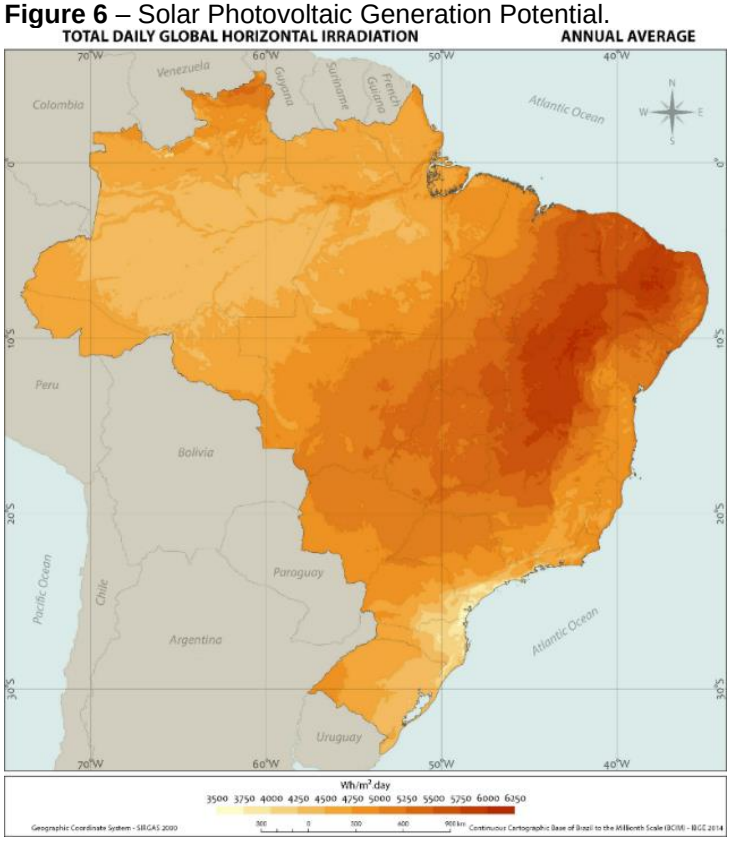

Source: Adapted from the Brazilian Solar Energy Atlas (PEREIRA et al, 2017).

Figure 7 – Global Horizontal Irradiation – Germany.

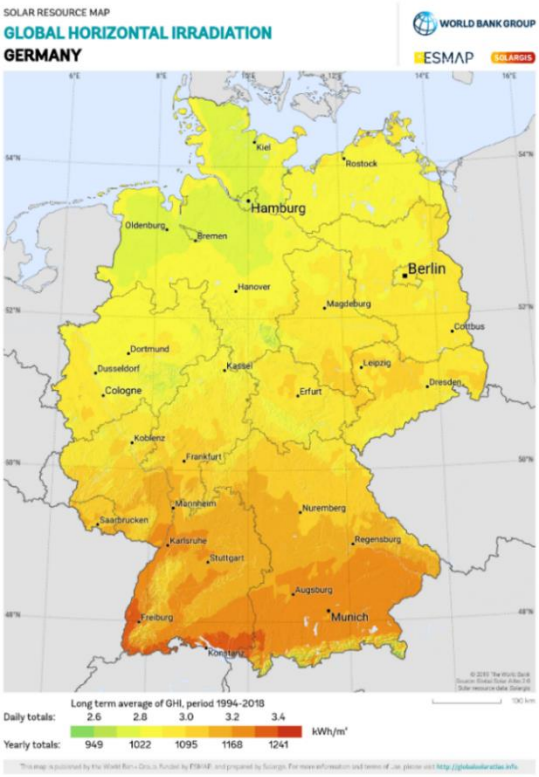

Source: © 2019 The World Bank, Source: Global Solar Atlas 2.0, Solar resource data: Solargis. Available from <https://globalsolaratlas.info/download/germany>.

Figure 8 represents the Brazilian photovoltaic solar generation potential map, which shows the annual energy yield in kilowatt-hours and kilowatts-peak – kWh and kWp. It can be noted that the northeast and central-west regions of Brazil have the greatest potential for photovoltaic energy generation.

Focusing on the study area of this work, the State of Paraná presents means of solar irradiation superior to several European countries (Fig.9). According to the Solar Atlas of the State of Paraná (2017), only six European countries had higher solar irradiation and photovoltaic productivity averages than the State of Paraná (TIEPOLO *et al.*, 2017). Figure 9 shows the State of Paraná compared to European countries, with the annual irradiation in kWh/m² and respective yield in kWh/kWp.year.

Figure 8 – Solar Photovoltaic Generation Potential.

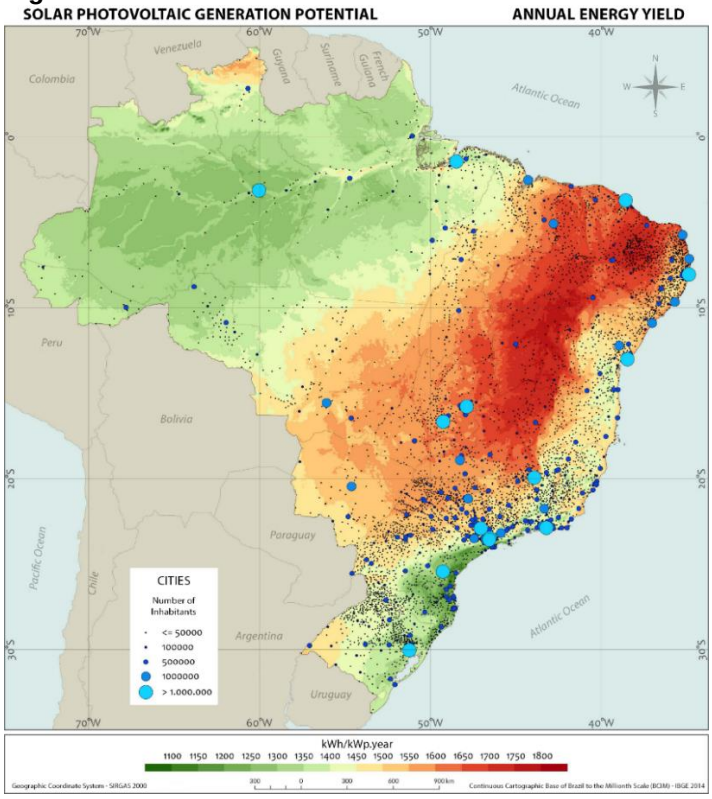

Source: Adapted from the Brazilian Solar Energy Atlas (PEREIRA et al, 2017).

Figure 9 – Comparison of State of Paraná Irradiation and European Irradiation

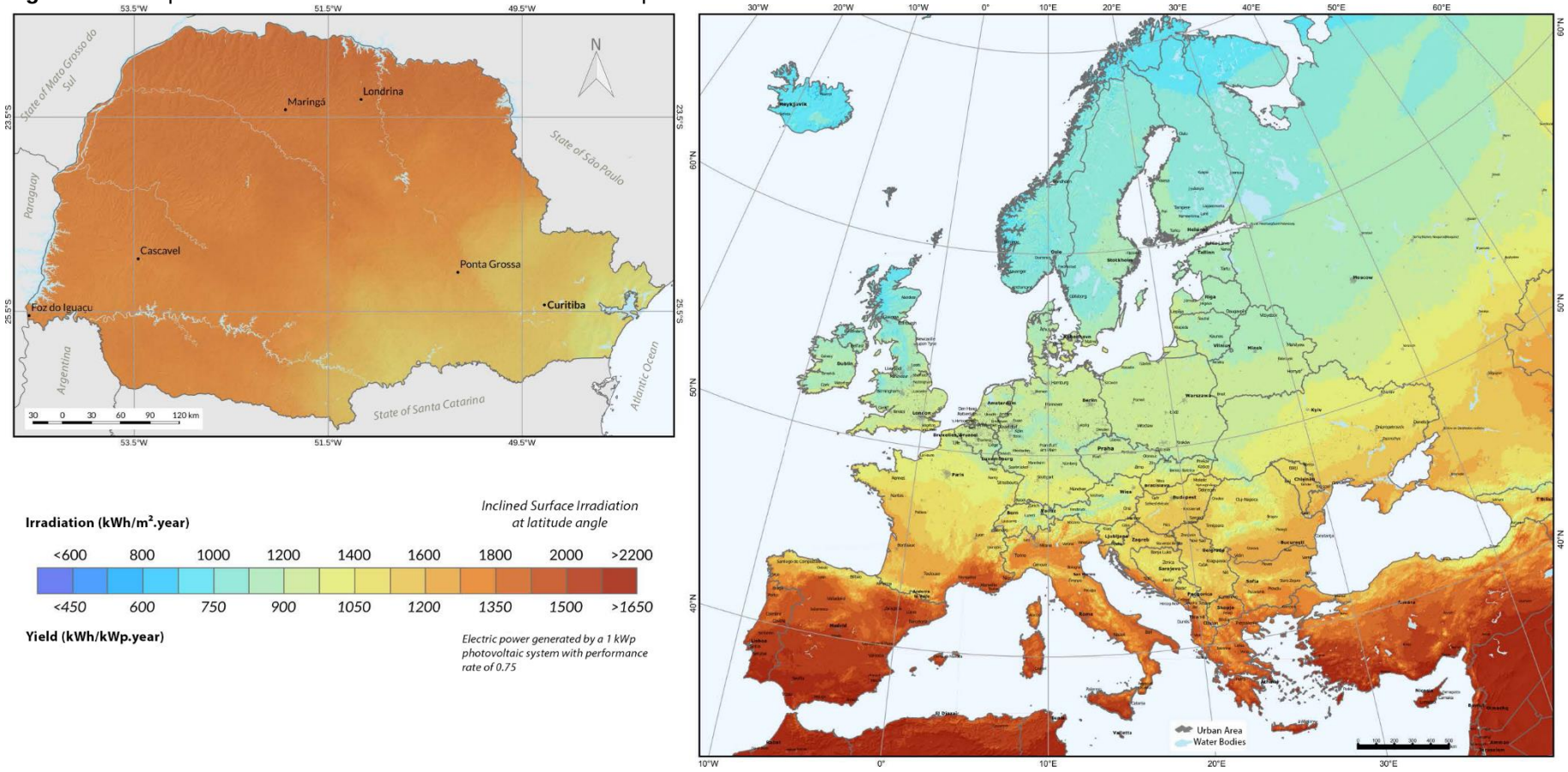

Source: Adapted from the State of Parana Solar Atlas (TIEPOLO et al, 2017).

4 ARTICLE 1 - EFFECTS OF A FLOATING PHOTOVOLTAIC SYSTEM ON THE WATER EVAPORATION RATE IN THE PASSAÚNA RESERVOIR

ABSTRACT

Freshwater scarcity is a significant concern due to climate change in some regions of Brazil; likewise, evaporation rates have increased over the years. Floating photovoltaic systems can reduce water evaporation from reservoirs by suppressing the evaporating area on the water surface. This work evaluated the effects of the floating photovoltaic system on water evaporation rates in the Passaúna Reservoir in southeastern Brazil. Meteorological data such as temperature, humidity, wind speed and solar radiation were used to estimate the rate of water evaporation using FAO Penman-Monteith, Linacre, Hargraves-Samani, Rohwer, and Valiantzas methods. The methods were compared with the Kruskal-Wallis test, including measured evaporation from the nearest meteorological station to determine whether there were significant differences between the medians of the methods considering a 95% confidence level for hypothesis testing. All methods differed from the standard method recommended by FAO Penman-Monteith. Simulations with more extensive coverage areas of the floating photovoltaic system were done to verify the relationship between the surface water coverage area and the evaporation reduction efficiency provided by the system and to obtain the avoided water evaporation volume. An efficiency of 60.20% was obtained in reducing water evaporation with a coverage area of 1265.14 m^2; it was also considered expansions of the FPS with coverage areas corresponding to energy production capacities of 1 MWp, 2.5 MWp and 5 MWp. The results indicated that for a floating photovoltaic system coverage area corresponding to 5 MWp of energy production capacity, the accumulated saved water volume would be enough to supply over 196 people for a year. More significant areas, such as covering up the entire available surface area of the Passaúna reservoir with a floating photovoltaic system, could save up to 2.69 hm^3 of water volume annually, which would represent a more significant value for the public management of water resources.

Keywords: Water Evaporation. Floating Photovoltaic System. Climate Changes.

4.1 INTRODUCTION

Water scarcity is one of the most relevant aspects of the world stage. With the growing demand for water resources - which are used for the most diverse purposes, from the primary to the tertiary sector – their practical use is vital for human life and the economy, especially knowing that it is a limited resource. Water reservoirs are crucial in the development of water resources management policies, as well as a way to control variations in water availability in periods of drought and floods.

Alternatives to optimize the use of water resources are increasingly necessary with the growing environmental concern and also the need for the rational use of water. Craig (2005a) estimates that half of the water in reservoirs is lost through evaporation. Bontempo Scavo *et al.* (2020) also highlight this issue, evaporative water losses are likely to increase in the coming years due to global warming, and solutions to maximize the use of water resources are essential.

The water surface evaporation in reservoirs represents an essential value for controlling water output, being one of the ways of monitoring water resources (WURBS; AYALA, 2013). Studies of water evaporation in reservoirs can be used to understand how global average temperatures change the amount of water lost through evaporation. In warmer climates and rising temperatures, water evaporation losses also increase (HELFER; LEMCKERT; ZHANG, 2012; HARTMANN, 2016).

Researches on water evaporation estimation in lakes and reservoirs date back to the beginning of the 20th century. It is quantified by a variety of meteorological data, such as incidence of solar radiation, wind speed, relative humidity, air temperature, and atmospheric pressure. In addition, it is a variable that is difficult to obtain directly, which is why methods for indirect estimates have been developed (HARWELL, 2012; CURTARELLI *et al.*, 2013).

Different methods based on meteorological data and empirical evapotranspiration equations have been used to estimate water evaporation from lakes and reservoirs (PEREIRA, 2004; CRAIG, 2005b; VALIANTZAS, 2006; HELFER; LEMCKERT; ZHANG, 2012; MCMAHON *et al.*, 2013; KOHLI; FRENKEN, 2015; HASSAN *et al.*, 2015; VIEIRA, *et al.*, 2016; TABOADA *et al.*, 2017; COELHO *et al.*, 2018; BONTEMPO SCAVO *et al.*, 2020; HAAS *et al.*, 2020; RODRIGUES; RAMALHO; MEDEIROS, 2020).

A method based on aerodynamics, mainly considering wind speed, was one of the first attempts to estimate water evaporation through an empirical equation (ROHWER, 1931). This study was based on the need to determine the feasibility of irrigation water reservoirs considering evaporative losses.

The Food and Agriculture Organization of the United Nations (FAO) standardized the Penman-Monteith method (PENMAN, 1948; MONTEITH, 1965; ALLEN *et al.*, 1998), which determines the reference evapotranspiration of the crop. However, Kohli; Frenken (2015) state that when using a crop coefficient value as one, the FAO Penman-Monteith method would lead to water evaporation in reservoirs. Data such as air temperature, humidity, solar radiation, and wind speed are required for this method.

The FAO Penman-Monteith method requires many data and an intensive calculation step. Other methods have been proposed as a simplified version of the FAO Penman-Monteith method, such as Linacre (1977), which is based on data of air temperature and local elevation; Linacre (1993), which includes air temperature, wind speed and solar radiation; Valiantzas (2006) that considers all variables such as solar radiation, air temperature, wind speed, and relative humidity. Allen *et al.* (1998) also recommend using an evapotranspiration equation when it is difficult to obtain enough climatological data, the Hargreaves-Samani equation, which depends on the maximum and minimum air temperature (HARGREAVES; SAMANI, 1985).

For that reason, the availability of different methods and their different variables or input data are important to estimate water evaporation, making their need notable when direct measurements are not available and when there is not enough data to use complex models like the FAO Penman-Monteith.

Reducing water evaporation in reservoirs is also important when considering the security of water availability - mainly in arid regions. It is possible to relate the reduction of evaporation with the water surface covered in reservoirs by floating photovoltaic systems, for example (AMINZADEH; LEHMANN; OR, 2018; ALTHOFF; RODRIGUES; SILVA, 2020).

Evaporation loss in reservoirs is a challenge for the efficient management of water resources, especially in regions with water scarcity (YAO, 2010). Studies have shown that devices such as floating or suspended covers can reduce the water evaporation rates by up to 90% (CRAIG, 2005b; HASSAN *et al.*, 2015; TABOADA *et al.*, 2017; CAZZANIGA *et al.*, 2018). Thus, floating photovoltaic systems can be a

solution to mitigate water losses by evaporation in reservoirs. Floating photovoltaic systems (FPS) can be used for water management by reducing water evaporation rates, producing energy, and reducing algae growth by improving the water quality (HAAS *et al.*, 2020; BONTEMPO SCAVO *et al.*, 2020).

Previous studies on the efficiency of FPS in reducing water evaporation have shown that flexible modules can reduce evaporation rates by 42% to 64%, with areas covered with FPS from 30% to 50% of the reservoir surface (BONTEMPO SCAVO *et al.*, 2020).

This work presents comparative results of the effects of an FPS installed in the Passaúna reservoir on the water evaporation rates using different water evaporation methods. It also evaluates the volume of water saved with future expansions of the energy production capacity resulting from the reduction of water evaporation due to the increase in the coverage area of the FPS. The decrease in evaporation losses due to the installation of the FPS can contribute to the amount of available water used to supply the local population or for other purposes.

4.2 METHODS

4.2.1 Case study site

The Passaúna Reservoir originated from the damming of the Passaúna River in 1990. It is located southwest of Curitiba in Paraná State, South of Brazil (Figure 10).

The reservoir has a surface area of 8.5 km², a maximum depth of 18.1 m, an average depth of 6.5 m, and a useful volume of 48 hm³ (SANEPAR, 2013; CARNEIRO; KELDERMAN; IRVINE, 2016; SOTIRI *et al.*, 2021).

According to Sotiri *et al.* (2021) the Passaúna Reservoir has a storage capacity of 69.3 hm^3 and a dead volume of 19.5 hm^3. The reservoir borders the cities of Curitiba, Araucária, and Campo Largo, and supplies 20% of the water demand consumed by the population of the metropolitan region of Curitiba (SANEPAR, 2013; SALES, 2020; GOLYJESWSKI; 2020).

Figure 10 – Location of the Passaúna Reservoir

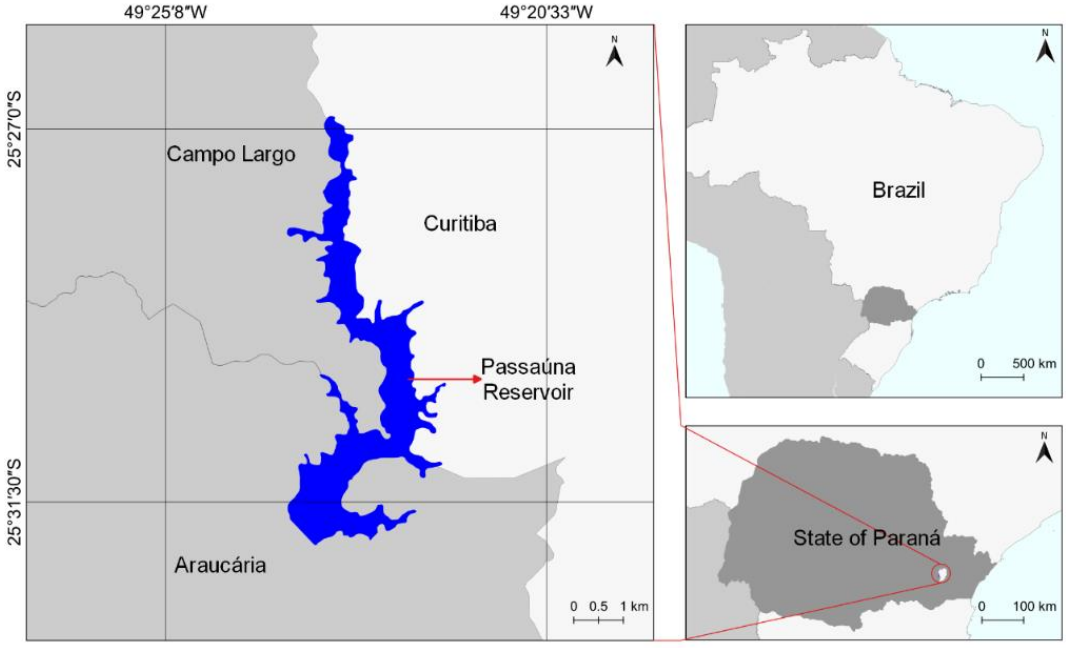

Geographic Coordinate System – SIRGAS 2000
Cartographic Base: Sudhersa, 2011; IPPUC, 2011; IBGE, 2017.

Source: The author.

4.2.2 Floating photovoltaic system (FPS)

The FPS was installed in 2019 in the Passaúna Reservoir (Figure 11), with an energy production capacity of 130 kWp, occupying an area of 1265.14 m² with 396 photovoltaic modules installed on a floating platform. It is located close to the water supply pumping system of the Water and Sanitation Company of Paraná (Sanepar), at the coordinates 25º30'45" S and 49º22'07" W (Figure 12).

The modular floating devices from the FPS can be easily removed or added, with the possibility of expanding the system in the future. The floating platform supports the photovoltaic modules, which have dimensions of 1960 mm x 991 mm x 40 mm and a maximum power of 330W each (JA Solar, 2022)[1]. The FPS consists of 22 strings, and each string contains 18 photovoltaic modules. Every two strings, there is an access walkway for module maintenance.

[1] Available from: <https://www.jasolar.com/>. Access on 15 Feb. 2022.

Figure 11 – Floating Photovoltaic System in the Passaúna Reservoir

Source: Sanepar (2019)[2].

Figure 12 – Aerial view of the Floating Photovoltaic System and the water pumping system

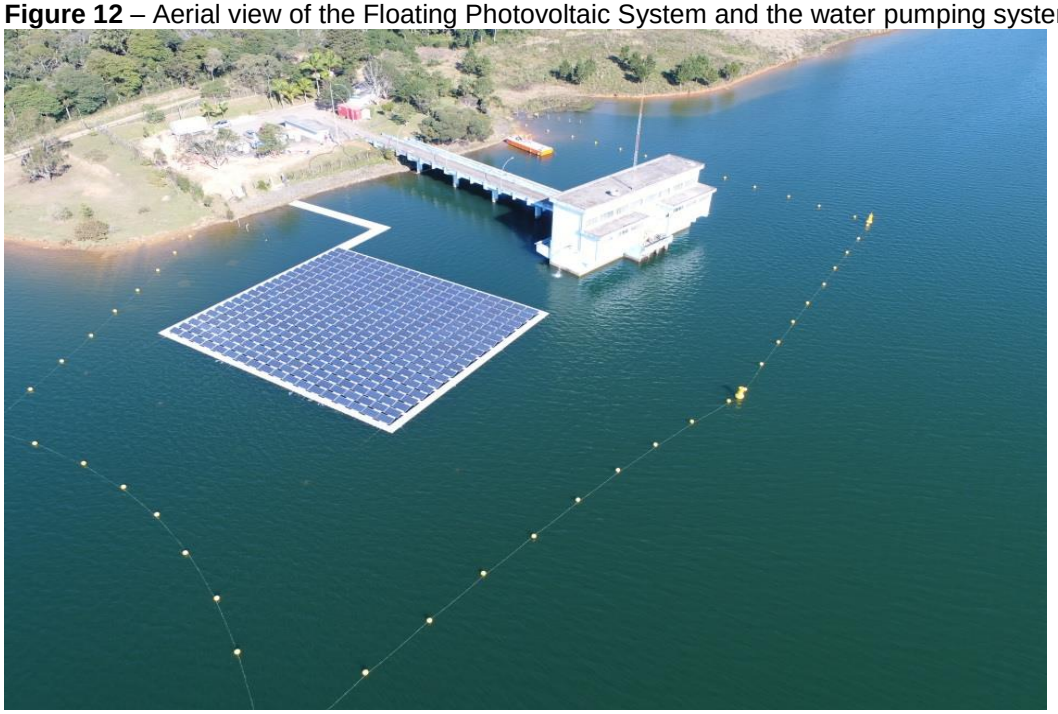

Source: Sanepar (2019)[3].

[2] Available from: <http://site.sanepar.com.br/noticias/governo-do-pr-e-sanepar-inauguram-obras-em-curitiba>. Access on 22 Feb. 2021.

4.2.3 Meteorological Data

The meteorological dataset used for this work was obtained from the weather station installed close to the FPS site. The input data, from 1st July 2020 to 30th June 2021, to obtain evaporation by the methods studied were: solar radiation, air temperature, relative humidity, and wind speed. Data gaps were observed in October (3rd to 16th and 25th to 30th), November (27th to 29th), and December (3rd).

In order to have continuous data over the period, the missing data were filled through linear regression with data from another meteorological station located 14 km from the Passaúna Reservoir. These data are available in the Meteorological Database for Teaching and Research (BDMEP) of the National Institute of Meteorology (INMET).

The measured evaporation data, which uses a Piché evaporimeter with daily resolution, were obtained from the INMET meteorological station for the same period. Non-continuous monthly failures were observed in the measured evaporation data.

4.2.4 Evaporation estimative

The methods used to estimate water evaporation to assess the influence of the FPS on the Passaúna reservoir were: FAO Penman-Monteith, Linacre (1977), Linacre (1993), Rohwer, Valiantzas, and Hargreaves-Samani - as described in the literature review. The results obtained from the methods were compared with the evaporation measured from the INMET meteorological station. Data were analyzed monthly in R-Studio 1.4.17 (RSTUDIO TEAM, 2020). In addition to comparing the results obtained by the methods and the measured evaporation values, linear regression and Pearson's correlation coefficient were calculated to understand the relationship between the FAO Penman-Monteith standardized method and other estimation methods.

The estimated evaporations were analyzed using the non-parametric Kruskal-Wallis test to determine whether there were significant differences between the medians obtained from the methods, with a 95% confidence level for hypothesis testing.

In order to estimate the efficiency of reducing water evaporation by the FPS, the Assouline; Narkis; Or (2011) method was used.

Equation (34) was used to estimate the daily evaporated volume in the reservoir:

$$T_{vol}=(E)(A)10^{3} \quad (34)$$

Where:

T_{vol} = daily evaporated volume (m^3)

E = evaporation rate ($mm\ day^{-1}$)

A = reservoir area (km^2)

The sum of each value of daily evaporated volume for a respective month can result in the monthly evaporated volume.

To evaluate future expansions of the FPS and its influences on the evaporation rates in the Passaúna reservoir, the water volume that could be lost by evaporation but would be avoided by the FPS was obtained. For the calculations, the current coverage area (130 kWp) was considered, and those corresponding to the expansions of energy production capacity of 1 MWp, 2.5 MWp and 5 MWp. These expansions were determined in accordance with ANEEL normative resolution 482/2012, which limits renewable energy mini-generation systems to 5 MWp (ANEEL, 2012).

The evaporated volume avoided by different coverage areas of the FPS was obtained by the equation (35):

$$\Delta=(T_{vol})(EQC)(\varepsilon) \quad (35)$$

Where:

Δ = avoided evaporation volume for assumed coverage (m^3)

T_{vol} = daily evaporated volume (m^3)

EQC = equivalent covered area for each energy production capacity (m^2)

ε = assumed evaporation reduction efficiency (%)

The available surface area of the reservoir was considered for the total storage volume and the volume during periods of water scarcity.

4.3 RESULTS AND DISCUSSION

4.3.1 Meteorological dataset

Figure 13 shows the variation of meteorological data from the weather station close to the FPS, used to estimate the evaporation rates from the different methods. The meteorological dataset refers to the period of one year, from 1st July 2020 to 30th June 2021.

Figure 13 – Weather data for the study site (July 1st, 2020 to June 30th, 2021).

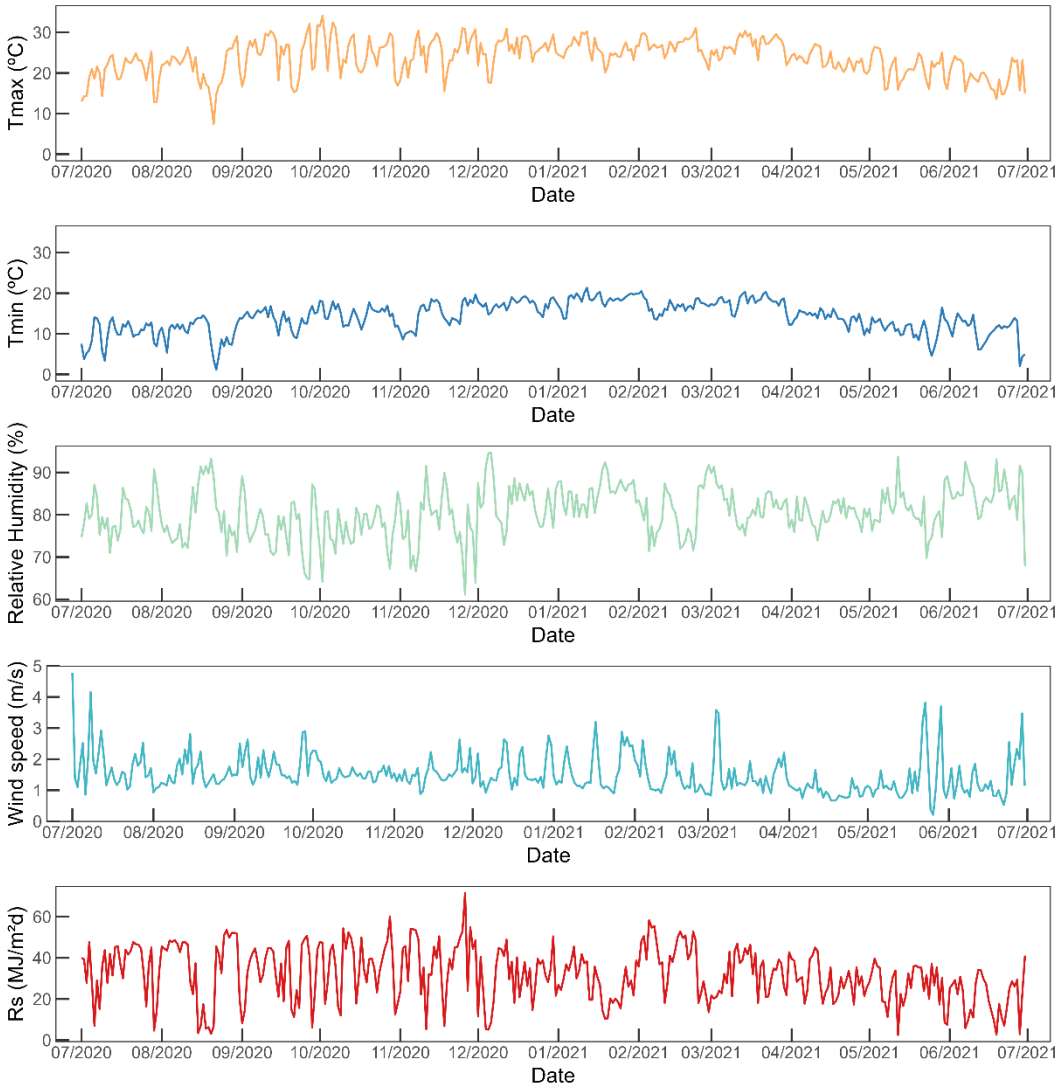

Source: The author

It was observed from the dataset a maximum temperature of 34.13 ºC and a minimum temperature of 1.14 ºC. The relative humidity ranges from 61.12% to

94.72%, and wind speed from 0.21 m s^{-1} to 4.16 m s^{-1}. The solar radiation average for the region is 31.96 MJ m^{-2} day^{-1} or 369.91 W m^{-2}.

4.3.2 Evaporation rates by the comparison of the methods

Table 2 presents the average and standard deviation evaporation rates for the methods studied and the measured evaporation data.

Table 2 – Comparative table showing the mean and standard deviation for six evaporation methods and measured evaporation.

Month	Evaporation (Mean ± SD) (mm day^{-1})						
	Measured Evap.	**Penman-Monteith**	**Linacre (1977)**	**Rohwer**	**Valiantzas**	**Hargreaves-Samani**	**Linacre (1993)**
Jul.	2.24±0.95	1.19±0.43	2.47±0.45	3.51±1.32	6.14±1.95	5.68±1.15	22.66±9.78
Aug.	1.94±1.24	1.23±0.54	2.53±0.55	3.66±1.79	6.66±3.03	6.85±1.97	23.79±13.96
Sept.	2.33±1.33	1.81±0.81	3.18±0.66	5.59±2.85	7.74±3.21	9.01±2.46	26.96±14.28
Oct.	3.24±2.10	1.93±0.73	3.32±0.63	5.29±2.37	8.66±3.02	10.03±2.23	31.01±13.93
Nov.	2.3±1.27	1.97±0.97	3.25±0.79	4.9±2.33	9.12±3.71	10.23±2.26	33.04±17.32
Dec.	2.43±0.95	1.65±0.68	3.19±0.44	4.21±1.79	7.44±3.01	9.83±2.02	25.97±13.29
Jan.	1.87±0.77	1.54±0.53	3.18±0.35	3.83±1.31	6.94±2.32	9.09±1.56	23.96±10.45
Feb.	2.94±1.18	1.99±0.69	3.41±0.45	4.64±1.53	9.48±2.98	10.41±1.60	35.92±13.56
Mar.	1.94±0.71	1.68±0.44	3.3±0.36	4.53±1.14	7.78±2.03	9.28±1.22	28.54±9.79
Apr.	1.81±0.33	1.12±0.34	2.9±0.29	3.14±0.82	5.95±1.69	7.43±1.16	21.38±7.85
May	2.15±0.81	0.99±0.46	2.57±0.41	3.03±1.29	5.05±1.84	6.16±1.39	17.63±8.58
Jun.	1.12±0.63	0.71±0.30	2.22±0.33	2.4±1.03	3.74±1.55	4.89±1.27	12.22±7.33
Annual cumulated evaporation (mm $year^{-1}$)	566.30	538.59	1074.93	1475.8	2559.60	2994.78	9165.54

Source: The author.

The results obtained by the FAO Penman-Monteith method slightly underestimated the evaporation, while the results of annual evaporation rates obtained by the Linacre (1977), Rohwer (1931), Valiantzas (2006), Hargreaves-Samani (1985), and Linacre (1993) methods were overestimated.

In a numerical comparison study of accumulated evaporation by evaporation methods and data measured in Catania - Italy, the Penman-Monteith and Hargreaves-Samani methods slightly underestimated the evaporation rates, while Valiantzas and Rohwer methods slightly overestimated the evaporation values. The study concluded that all methods could be used in the long-term analysis. However, better short-term results are obtained using more complex models such as the Penman-Monteith (BONTEMPO SCAVO *et al.*, 2020).

The results of the Kruskal-Wallis test for comparing methods and measured evaporation are shown in Table 3.

Table 3 – Kruskal-Wallis test results for the evaporation values obtained by the methods and measured evaporation values.

Method	Jul.	Aug.	Sept.	Oct.	Nov.	Dec.	Jan.	Feb.	Mar.	Apr.	May	Jun.
Measured Evap.	c	de	de	d	de	d	e	d	f	e	b	c
Penman-Monteith	d	e	e	e	e	d	e	e	f	f	c	c
Linacre (1977)	bc	cd	d	d	cd	c	d	cd	e	d	b	b
Rohwer	b	bc	c	c	c	c	d	c	d	d	b	b
Valiantzas	a	ab	b	b	b	b	c	b	c	c	a	a
Hargreaves-Samani	a	a	ab	ab	ab	ab	b	b	b	b	a	a
Linacre (1993)	a	a	a	a	a	a	a	a	a	a	a	a

Note: Methods with the same letter are not significantly different from each other at $p < 0.05$ by the Kruskal-Wallis test.
Source: The author.

Based on the results in Table 3, the evaporation values obtained by the Linacre (1997) and Penman-Monteith methods were more similar to the measured evaporation values.

The Linacre method (LINACRE, 1977) did not differ statistically from the evaporation values measured in July, August, September, October, November (2020), February, and May (2021), with a confidence level of 95%.

The Penman-Monteith method (ALLEN *et al.*, 1998) did not differ statistically from the evaporation values measured in August, September, November, December (2020), January, March, and June (2021), with a confidence level of 95%.

The Rohwer method (ROHWER, 1931) did not differ statistically only in May from the evaporation values measured with a confidence level of 95%. The Hargreaves-Samani (HARGREAVES; SAMANI, 1985), Valiantzas (VALIANTZAS, 2006), and Linacre (1993) methods differed statistically from the measured evaporation for all months with a confidence level of 95%.

Linacre's (1993) method is an optimization of Linacre's (1977) early method, in which wind speed variations and a better approach to net radiation are included. The results obtained presented differences with a confidence level of 95%.

Linear regression showed that all estimation methods strongly correlated with the standardized Penman-Monteith method, the coefficient of determination (R^2) were between 0.707 - 0.901, and the Pearson correlation coefficient (r) was between 0.840 - 0.949, as shown in Figure 14.

Figure 14 – Linear regression between FAO Penman-Monteith and other methods

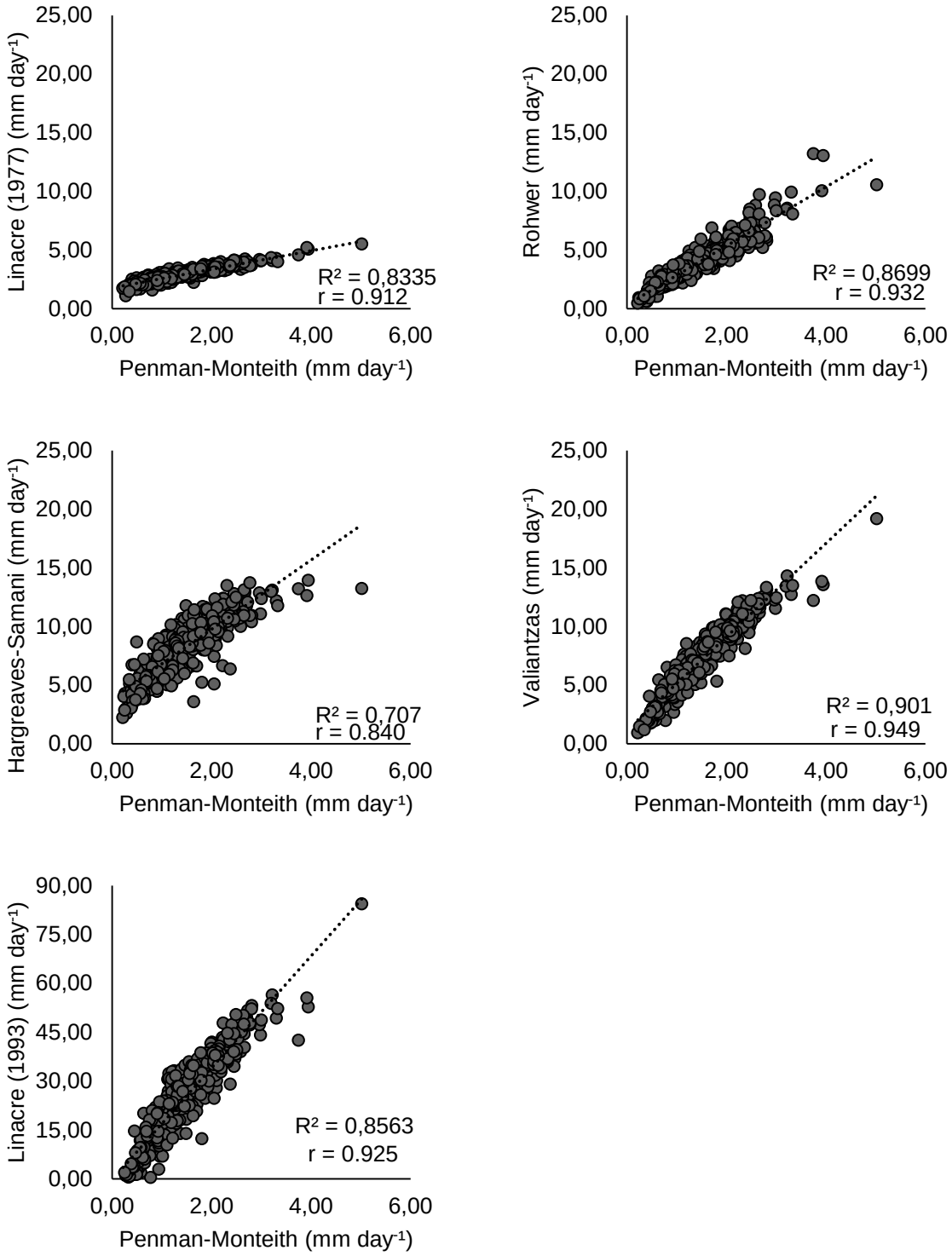

Source: The author.

Although the methods show a strong correlation, they do not reflect the climatic conditions of the Passaúna reservoir region. Implying that the methods are validated for specific climates; therefore, scale differences between the methods were shown (WURBS; AYALA, 2013).

Coelho *et al.* (2017) also found differences between the evaporation estimation methods, but with underestimated results for Linacre (1993) compared to the Penman-Monteith, different from the overestimation we obtained. This difference could be explained by the high rainfall rates during most of the year in Tucuruí – Northeast Brazil, leading to an underestimation of the solar radiation and, consequently, the evaporation rates.

Similar results were obtained for the Sobradinho and Três Marias reservoirs in Southeastern Brazil, in which the Linacre (1993) method overestimated the evaporation compared to the Penman-Monteith method (VIEIRA *et al.*, 2016; PEREIRA *et al.*, 2009).

The Valiantzas method (2006) showed better accuracy compared to the FAO Penman-Monteith method on a daily scale in southern China due to the consideration of the four variables of air temperature, relative humidity, wind speed and solar radiation, which are important meteorological parameters for estimating evaporation (LI *et al.*, 2018).

For the present work, the evaporation values obtained by the Linacre (1977), Penman-Monteith, and Rohwer methods were the closest to the measured evaporation values. The results of the evaporation rates estimated by these methods and the measured evaporation are presented in Figure 15.

Figure 15 – Comparison between estimated evaporation (mm day $^{-1}$) methods from Linacre (1977), FAO Penman-Monteith, Rohwer and the measured evaporation.

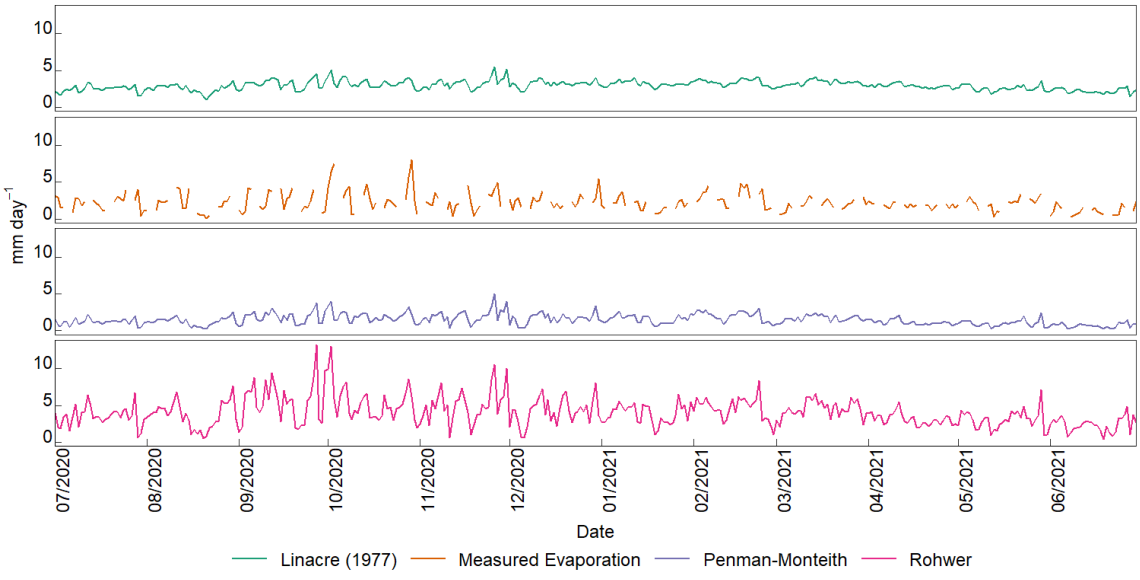

Source: The author.

Comparing the monthly evaporation results obtained by the methods and those measured, the Rohwer (1931) method has differed statistically in all months except May. Linacre's (1977) method differed statistically in December, January, March, April, and June. Moreover, the Penman-Monteith method (ALLEN *et al.*, 1998) differed statistically in July, October, February, April, and May, for all analyses, with a confidence level of 95%.

The FAO Penman-Monteith presented the best results, so it was chosen for calculating the evaporation estimate for different areas of the FPS, presented in the following items.

4.3.3 Floating Photovoltaic system water evaporation reduction

The FAO Penman-Monteith method was used to estimate the water evaporation in the Passaúna reservoir. Furthermore, its results were used to estimate the evaporation reduction considering the area covered by the FPS and its future expansions. The Assouline; Narkis; Or (2011) relation was implemented to obtain the reduction in the evaporation rates considering the interference of the FPS, as shown in Table 4.

Table 4 – Results of the Assouline; Narkis; Or (2011) evaporation reduction efficiency relation for the Floating Photovoltaic System.

Energy Production Capacity (MWp)	FPS area (m²)	FPS open area (m²)	α (evaporating fraction)	X	Ɛ (Small Openings)	Ɛ (Large Openings)
0.13	1265.14	199.83	0.157	0.842	0.602	0.707
1	9731.84	1537.15				
2.5	24329.62	3842.88				
5	48659.23	7685.76				

Source: The author.

As shown in Table 4, the FPS occupies a covered area of 1,265.14 m², with a total opening area of 199.83 m², resulting in an evaporation fraction of 0.157. Such value corresponds to a relatively small covered surface in relation to the total area of the reservoir – approximately 0.01%; therefore expansions of the FPS corresponding to energy production capacities of 1 MWp, 2.5 MWp and 5 MWp were calculated, maintaining the openings and coverage ratio of the photovoltaic modules and their surrounding of area. The efficiency was estimated from 60.20% to 70.70% for the

evaporation reduction by the FPS. The most conservative (60.20%) was assumed to estimate the evaporation reduction.

The available area of the reservoir was presumed in two approaches: reservoir area at its total volume of water storage with an area of 8.5 km², and another with the current available area of 6.95 km² considering the water scarcity period as shown in Figure 16.

Figure 16 – Aerial view of the water surface area of the Passaúna Reservoir and the FPS site during the water shortage in 2021.

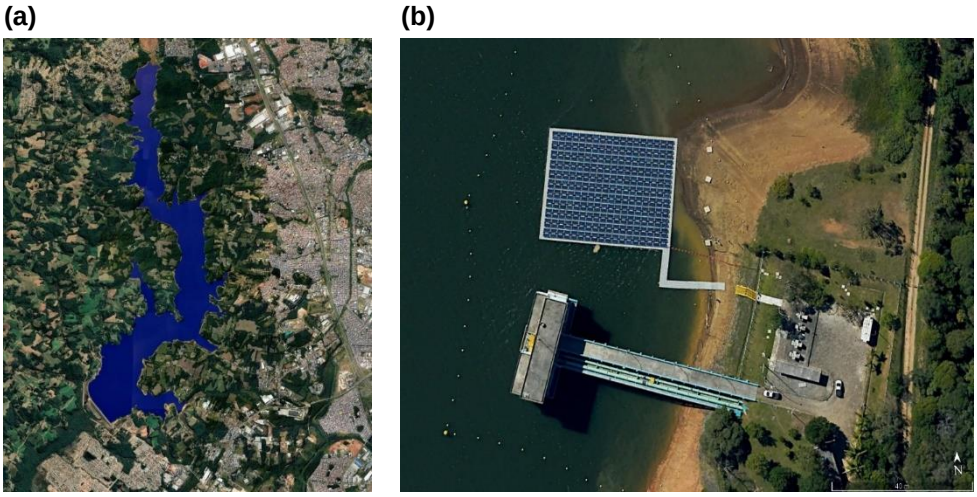

Note: (a) Passaúna Reservoir. (b) FPS site highlighting the low water level.
Source: The author (adapted from Google Earth images).

Figure 17 shows the annual daily behavior of evaporated water volume in the Passaúna reservoir considering the period of water scarcity.

Figure 17 – Annual daily volume of evaporated water in the Passaúna reservoir.

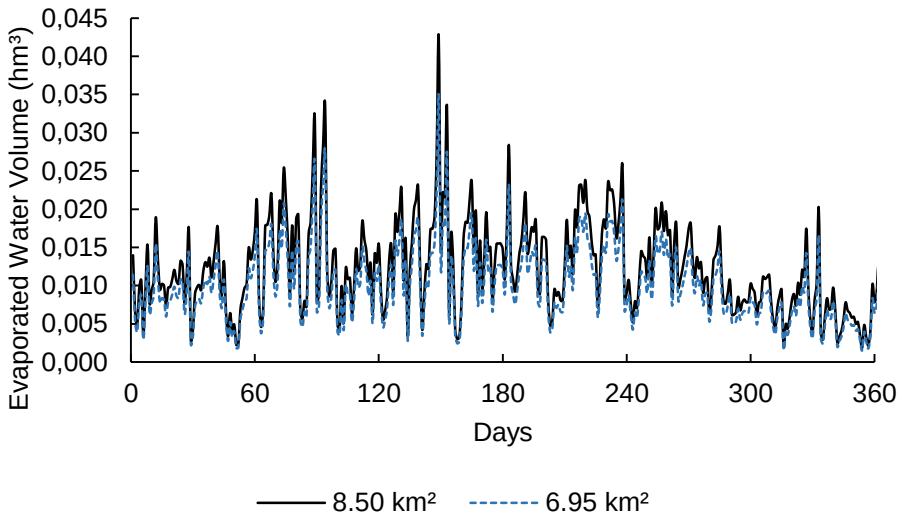

Source: The author.

The highest values of evaporated water volume, observed in Figure 17, were in summer, followed by spring, autumn and winter. For the surface area of the Passaúna reservoir, considering the total storage volume, the accumulated volume of evaporated water during the year is 4.47 hm³. Considering the surface area in the period of water scarcity, the volume of evaporated water is 3.65 hm³. In terms of the average volume of water used by Sanepar in 2021 (43 hm³) to supply the population, these volumes correspond to approximately 10.4% and 8.5%, respectively. The accumulated volume of evaporated water could supply 58,596 and 47,846 people by year, respectively.

Figure 18 shows the accumulated volume of water saved by covering the water surface occupied by the FPS current area and area expansions corresponding to an energy production capacity of 1 MWp (A1), 2.5 MWp (A2), and 5 MWp (A3).

Figure 18 – Accumulated saved water volume by the FPS for the current area and future expansions.

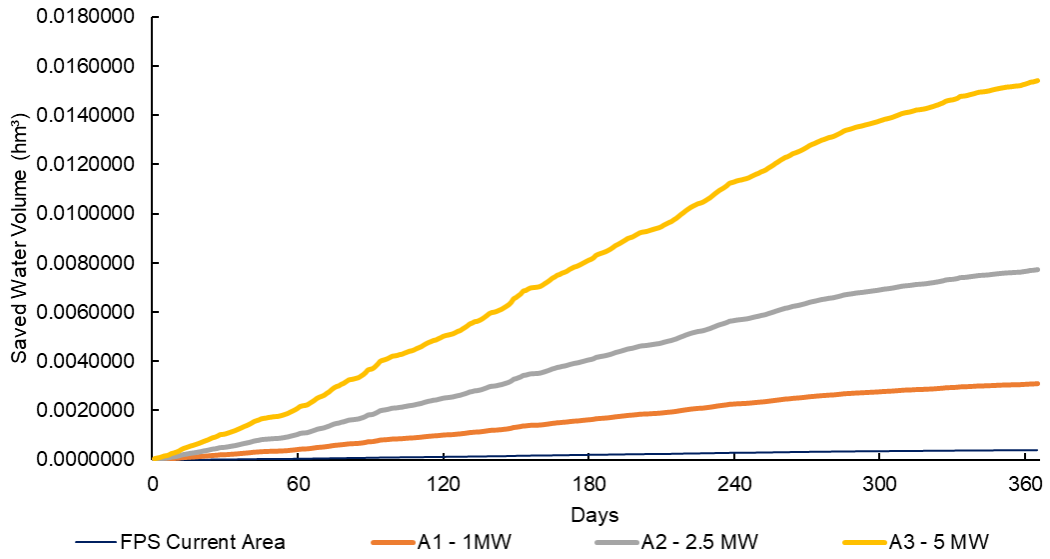

Source: The author.

Figure 18 shows that the larger the area of the FPS on the water surface, the more significant the reduction of the water evaporation and, consequently, the greater the volume of the saved water.

Although larger areas represent a more significant reduction of the water evaporation, the FPS occupies a small area in relation to the total surface area

available in the Passaúna Reservoir. The volume of water that can be saved by evaporation is approximately 0.015 hm^3 for the largest area (A3).

Considering a per capita water consumption of 0.209 m^3 per inhabitant per day, according to Sanepar in 2021, the accumulated volume of water saved by evaporation for an FPS with energy production of 5MWp would be enough to supply more than 196 people per year. In the same way, the FPS could supply the electricity demand for 2,564 inhabitants, considering the average per capita consumption of 1.95 kWh in the State of Paraná (EPE, 2022)[3].

Valadares (2017) evaluated the impact of FPS installed in reservoirs used for hydroelectric power generation on the evaporation rate in Brazil. The annual accumulated volume of water saved can approximate the total volume of water evaporated in a single day on the reservoir. The reduction in water evaporation due to the installation of the FPS was insignificant, especially when comparing the avoided evaporation in a water volume of 0.35 hm^3 with the total volume of the reservoir (792 hm^3), which could supply 6,304 people over a year.

Lopes *et al.* (2020) studied the evaporation reduction efficiency from the percentage of the coverage area over the total surface of the reservoir located in the Brazilian semiarid region. They concluded that the FPS had a relevant impact on the evaporation rate of weirs. They obtained similar results for different scenarios of covered areas, 19.4%, 50% and 70% of the weir surface, which can represent a reduction in the annual government expenses of 13.38%, 14.36%, and 15.3%, respectively, with a decrease in the water demand from water trucks, delivered to the population. The unevaporated water volumes per year obtained by the authors were 21.2%, 37% and 55.2% for covered areas of 30%, 50% and 70%, respectively.

Bontempo Scavo *et al.* (2020) obtained a 42% reduction in evaporation with flexible modules installed directly on the water, a system similar to the one installed in the Passaúna reservoir. In addition, the full coverage FPS below the modules presented a 49% reduction of water evaporation, showing that the greater the area covered by the FPS, avoiding exposure to the water surface, the more significant the decrease in water evaporation.

[3] Available from: <https://www.epe.gov.br/>. Access on 15 Jul. 2022.

4.4 CONCLUSION

For the design of the FPS, meteorological data to estimate the evaporation rates in reservoirs are important to avoid water losses, mainly in regions with water scarcity in long periods of drought.

As preliminary research on the effects of the FPS on estimating the evaporation rate in the Passaúna reservoir, the FAO Penman-Monteith and Linacre (1977) methods presented results closer to the measured evaporation.

The water evaporation reduction efficiency obtained considering the covered area of the FPS was 60.20%. FPS can effectively reduce the reservoir evaporation rate, where their coverage area over water occupies larger areas of the reservoir, which is not the case with the FPS installed at the Passaúna reservoir.

The water savings promoted by the current FPS area in the Passaúna reservoir and its future expansions to areas corresponding to energy productions of 1 MWp, 2.5 MWp and 5 MWp did not result in a significant volume in relation to the total surface available in the reservoir. Nevertheless, the water saved by evaporation could supply up to 196 people a year and about 2,564 people with electricity, considering per capita consumption of 209 L/day and 1.95 kWh, respectively.

The accumulated volume of evaporated water during one year was 4.47 hm^3, and in periods of water scarcity, this volume can be 3.65 hm^3. Considering the average volume of water withdrawn from the Passaúna reservoir by the Water and Sanitation Company in 2021 to supply the population was 43 hm^3. The accumulated volumes of evaporated water correspond to approximately 10.4% and 8.5%, respectively. The accumulated volume of evaporated water could supply 58,596 and 47,846 people annually, respectively. With an FPS covering the entire surface of the Passaúna reservoir, the volume of water saved could reach 2.69 hm^3, which could supply 35,262 people over a year, representing an essential value for the public management of the water resources in the reservoir.

5 ARTICLE 2 – EVALUATION OF FLOATING PHOTOVOLTAIC SYSTEMS ON THE EVAPORATION RATES IN RESERVOIRS AS A MITIGATION TO CLIMATE CHANGE

ABSTRACT

Freshwater scarcity is a significant concern due to climate change in some regions of Brazil; likewise, the water evaporation rates in reservoirs have increased over the years. A floating photovoltaic system was installed in the Passaúna Reservoir in southern Brazil. Studies indicate that installing floating photovoltaic systems can promote the reduction of evaporated water, which can result in a mitigation plan to save freshwater. The Water and Sanitation Company of Parana has been rationing the drinking water supply to the population due to the low levels of water in the reservoirs because of a long period of drought. In order to verify the effects of higher temperatures on the evaporation rates in the Passaúna reservoir, the PGECLIMA_R software was used to forecast scenarios from the Intergovernmental Panel on Climate Change (IPCC), using forecasted meteorological data for the years 2040, 2060, 2080, and 2100. It was possible to estimate the evaporation water losses using the FAO Penman-Monteith method and considering the temperature increase due to the climate change by the IPCC. Estimates of water evaporation were obtained for a floating photovoltaic system covering 30% and 70% of the surface area of the Passaúna reservoir to assess the volume of water saved. The estimated evaporation increased 11.59% and 31.88% for the year 2100 in SPP1-1.9 and SPP5-8.5, respectively. Water losses showed an increasing volume over the years by the end of the century, especially in later years; a difference of 29.78% is identified in the year 2100 between the optimistic and pessimistic scenarios. Considering an evaporation reduction efficiency of 60.20% by the coverage area of the floating photovoltaic system, and 18.06% to 42.14% water losses by evaporation can be prevented with a coverage area of 30% and 70%, respectively.

Keywords: Water Evaporation. Floating Photovoltaic System. Climate Changes.

5.1 INTRODUCTION

One of the problems when considering water scarcity is the evaporation losses, particularly in reservoirs – this may be due to the difficulty in obtaining consistent data, whether measured evaporation or consistent meteorological data, which can be used to estimate evaporation with different methods. The inconsistency of the flows calculated by historical series and the losses of water by evaporation in the reservoirs is an obstacle to managing water resources as reliable estimates are essential for water management (Pereira, 2004; Pereira *et al.*, 2009).

The Intergovernmental Panel on Climate Change (IPCC) was created to provide policymakers with regular scientific assessments of climate change, its implications and potential future risks and to present adaptation and mitigation options. There is evidence that the increase in greenhouse gas concentrations has caused an increase in global temperatures (IPCC, 2014).

New climate change scenarios were presented in the IPCC's recent Sixth Assessment Report, called Shared Socio-economic Representative Pathways (SSPs). They are based on the socio-economic development trend of anthropogenic factors of climate change. These scenarios range from low greenhouse gas (GHG) emissions (SSP1-1.9) to very high GHG emissions (SSP5-8.5) by the end of the 21st century. The SSPs were developed to complement the Represent Concentration Pathways (RCPs) scenarios from the Fifth Assessment Report (IPCC, 2021).

This study applied two extreme scenarios to simulate future climate change, one optimistic and the other pessimistic. For the optimistic scenario, an increase in the variation of the average air temperature of between 1.0ºC and 1.8ºC until 2100, was considered. For the pessimistic scenario, an increase of 3.3ºC to 5.7ºC was considered (IPCC, 2021).

The SSP narratives are described by O'Neill *et al.* (2017), in which the SPP1 or optimistic scenario would represent the economic and technological development associated with sustainable development, environmental awareness and sustainable consumption. In the SPP5 or pessimistic scenario, the dependence on fossil fuels and lack of environmental concern would prevail.

Based on the previous IPCC report, it is also possible to assume that an optimistic scenario would include rigorous mitigation of the reduction of the GHG emissions, as the pessimistic scenario would have no effort in this regard, climate

change would also increase the risk related to the water scarcity and droughts (IPCC, 2014). In this context, the increase in the global temperature would increase the evaporation rates in water bodies.

Previous studies have shown through climate simulations that in the future, with warmer temperatures, the evaporation rates also tend to increase. In a simulation carried out on a reservoir in Australia, Helfer *et al.* (2012) showed a significant increase in the evaporation rates for the periods 2030-2050 and 2070-2090, where an increase of 5.6% and 14.5% was observed, respectively.

Evaporation losses were also investigated in a reservoir in Iran; the predicted variations in the evaporation losses for the periods 2030-2050 and 2080-2100 were simulated with RCPs scenarios of the IPCC, in which the expected evaporation will likely increase in both simulated scenarios (Bazzi *et al.*, 2020). Climate change affects the air temperature and other parameters such as cloudiness and air humidity, influencing the water evaporation rates. Appropriate knowledge of the evaporation behavior would lead to assertive water management.

The FAO Penman-Monteith method has been widely used to estimate evaporation; it requires four variables: net radiation, wind speed, air temperature, and humidity (Donohue *et al.*, 2010). The method has been standardized by the Food and Agriculture Organization of the United Nations (FAO), and many studies have shown this method to be one of the closest estimated evaporation alternatives compared to directly measured evaporation (Helfer *et al.*, 2012; Taboada *et al.*, 2017; Scavo *et al.*, 2020).

Although climate change predicts an increase in the air temperature, it is not possible to state that this will induce an increase in water evaporation, as different variables affect the water evaporation indicating a complex interaction among the meteorological parameters (DONOHUE *et al.*, 2010; LIU; MCVICAR, 2012).

Bai *et al.* (2020) corroborate with the study of the authors above-cited, confirming that the decrease of the net radiation and wind speed contribute to the reduction of water evaporation. The study correlated atmospheric evaporation demand with actual evaporation, showing that a trend towards higher temperatures would not compensate for the decreases in the atmospheric evaporation demand due to solar radiation.

According to Virgens Filho *et al.* (2014), meteorological simulators such as PGECLIMA_R are designed to predict a synthetic series of meteorological data

correlated with historical series. PGECLIMA_R *software* performance has been studied and presented a high correlation between the predicted and observed meteorological data (VIRGENS FILHO *et al.*, 2014).

Climate change simulations can be used to observe different situations. PGECLIMA_R *software* can also be used to predict changes in the four variables of the evaporation under climate change scenarios from the IPCC.

Other researchers have already used PGECLIMA_R: to predict solar radiation and estimate the potential for photovoltaic generation in climate change scenarios (SGARBOSSA, 2019); simulate precipitation levels and predict impacts on rainwater storages (COSTA, 2016); study rainwater harvesting combined with photovoltaic energy in climate change scenarios (TSUNETO; VIRGENS FILHO, 2020).

The main objective of this work is to provide a preliminary study on the effects of a floating photovoltaic system on the evaporation rates in the Passaúna reservoir in different climate change scenarios, given the current concerns about sustainability and efficiency of the water resources management.

5.2 METHODS

5.2.1 Case study site

The floating photovoltaic system (FPS) is installed in the Passaúna reservoir in the southwest region of Curitiba in the Paraná State (Figure 19). The reservoir was originated from the damming of the Passaúna River in 1990; it has a surface area of 8.5 km², a maximum depth of 18.1 m, an average depth of 6.5 m, and a useful volume of 48 hm³ (SANEPAR, 2013; CARNEIRO; KELDERMAN; IRVINE, 2016; SOTIRI *et al.*, 2021).

The Passaúna reservoir borders the cities of Curitiba, Araucária, and Campo Largo; it is responsible for supplying about 20% of the population of the Metropolitan Region of Curitiba (SANEPAR, 2013; SALES, 2020; GOLYJESWSKI; 2020). The storage capacity of the reservoir is 69.3 hm³ with dead volume storage of 19.5 hm³ (SOTIRI *et al.*, 2021).

Figure 19 – Study Area Site

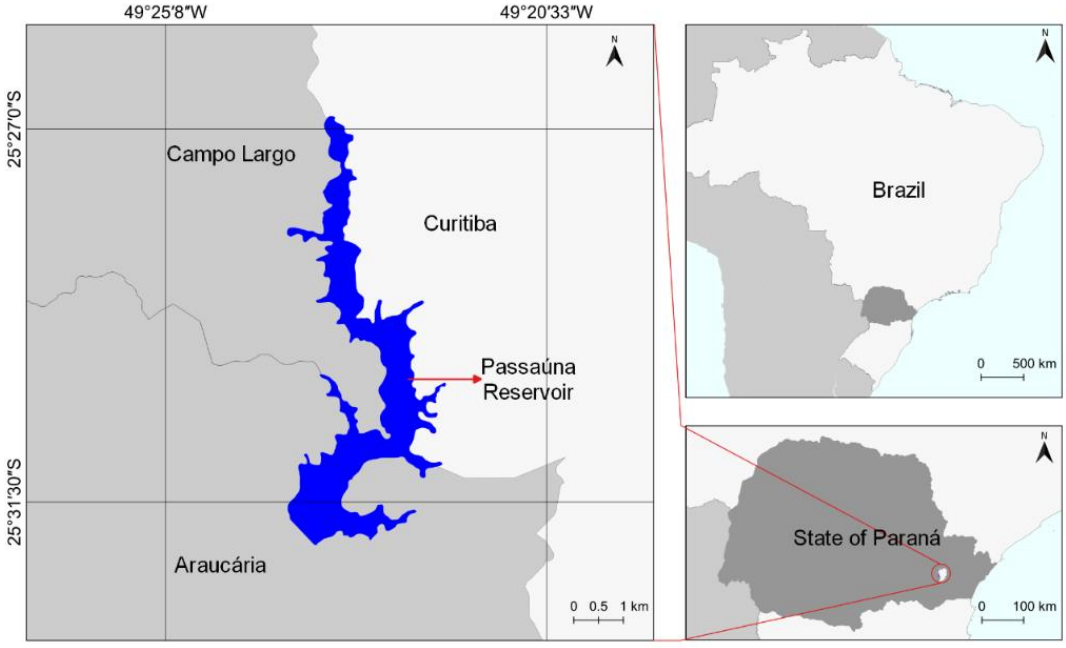

Geographic Coordinate System – SIRGAS 2000
Cartographic Base: Sudhersa, 2011; IPPUC, 2011; IBGE, 2017.
Source: The author.

5.2.2 Floating photovoltaic system

The FPS of the Passaúna Reservoir was installed in 2019, with an energy production capacity of 130 kWp, occupying an area of 1,265.14 m² with 396 photovoltaic modules, which are installed on a modular floating platform (Figure 20). It is located next to the pumping system for the water supply of the Water and Sanitation Company (Sanepar), at the coordinates 25º30’45” S and 49º22’07” W (Figure 21).

Figure 20 – Floating Photovoltaic System in the Passaúna Reservoir

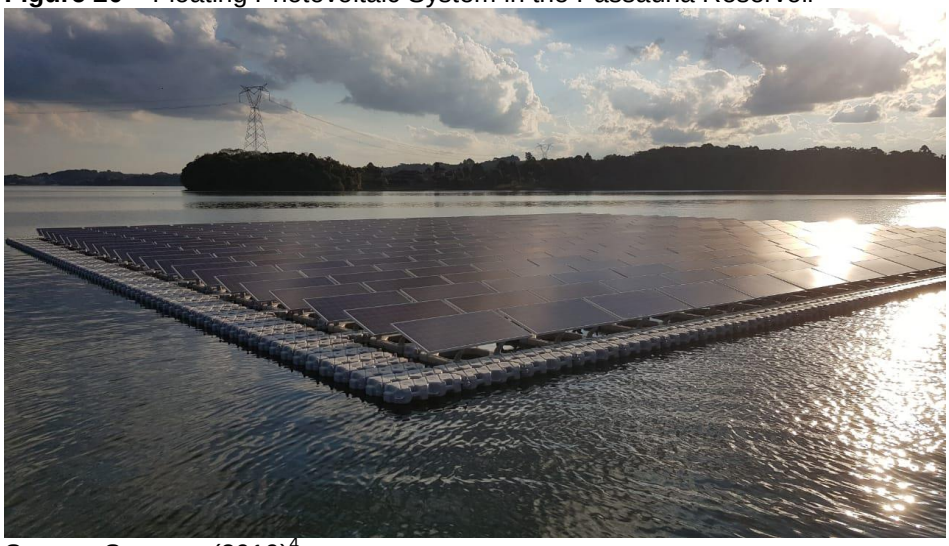

Source: Sanepar (2019)[4].

Figure 21 – Aerial view of the Floating Photovoltaic System and the water pumping system

Source: Sanepar (2019)[4].

5.2.3 Simulations of the climate change scenarios

Daily meteorological data from 1990 to 2020 were obtained from a meteorological station located 14 km from the Passaúna reservoir, available in the Meteorological Database for Teaching and Research (BDMEP) of the National Institute of Meteorology (INMET), considering this the database with longer and more consistent weather reports.

[4] Available from: <http://site.sanepar.com.br/noticias/governo-do-pr-e-sanepar-inauguram-obras-em-curitiba>. Access on 22 Feb. 2021.

From the database of INMET, meteorological simulations for the scenarios of the IPCC Sixth Assessment Report (2021) were simulated by the PGECLIMA_R, which resulted in the variables of air temperature, relative humidity, and solar radiation to the corresponding years 2040, 2060, 2080, and 2100. PGECLIMA_R is a computational tool that uses mathematical modelling through stochastic processes to generate daily climate data (Virgens Filho *et al.*, 2011a; Virgens Filho *et al.*, 2011b).

For the simulations of wind data, a beta probability distribution was used as presented by Falls (1973), the beta p and q parameters were obtained according to the methodology presented by Leite; Virgens Filho (2006, 2007), and Beruski *et al.* (2009).

Water evaporation losses were calculated using the Penman-Monteith method with the generated scenarios of meteorological data from the PGECLIMA_R. The used variables were air temperature, relative humidity and solar radiation – simulated by the PGECLIMA_R and the wind data simulated from a beta probability distribution. The influence of the area covered by the FPS on evaporation rates was determined using the Assouline; Narkis; Or (2011) equation to obtain the evaporation reduction efficiency.

To estimate the daily evaporated volume for the reservoir the following equation (36) was assumed:

$$T_{vol} = (E)(A)10^3 \quad (36)$$

Where:

T_{vol} = daily evaporated volume (m^3)

E = evaporation rate ($mm\ day^{-1}$)

A = reservoir area (km^2)

The sum of each value of daily evaporated volume for a respective month can result in monthly evaporated volume.

For corresponding coverage areas, the prevented evaporated volume by the Floating Photovoltaic System is obtained through the equation (37):

$$\Delta\% = (T_{vol})(\%C)(\varepsilon) \quad (37)$$

Where:

$\Delta\% = \text{avoided evaporation volume for assuming \% coverage } (\mathrm{m}^3)$

$\mathrm{T_{vol}} = \text{daily evaporated volume } (\mathrm{m}^3)$

$\%\mathrm{C} = \text{Covered area (percentage)}$

$\varepsilon = \text{assumed evaporation reduction efficiency (percentage)}$

5.3 RESULTS AND DISCUSSION

5.3.1 Present-day scenario (1991-2020)

According to the Köppen climate classification, the Passaúna reservoir region is in a humid subtropical zone – Cfb, characterized by a temperate summer and no dry season, with an average annual temperature of 17 ºC and annual rainfall of 1,550 mm (ALVARES *et al.*, 2014).

From the meteorological database from 1991-2020, the annual average temperature was 18 ºC, with average temperatures in summer and winter of 22 ºC and 16 ºC, respectively. Solar radiation in the region has higher values in summer and spring, with a mean annual value of 174 $W.m^{-2}$. The average wind speed over 30 years was 2 m/s.

During the observed period, the temperature had an increasing trend of 0.05 ºC per year, the relative humidity presented a decrease of -0.07 % per year, and the wind speed presented an increase of 0.005 m/s per year. The solar radiation did not change significantly, as shown in Figure 22.

Figure 22 shows the observed data from 1991 to 2020 of the variables required by the FAO Penman-Monteith method to obtain the evaporation rates.

Figure 22 – Observed data from the period 1991-2020.

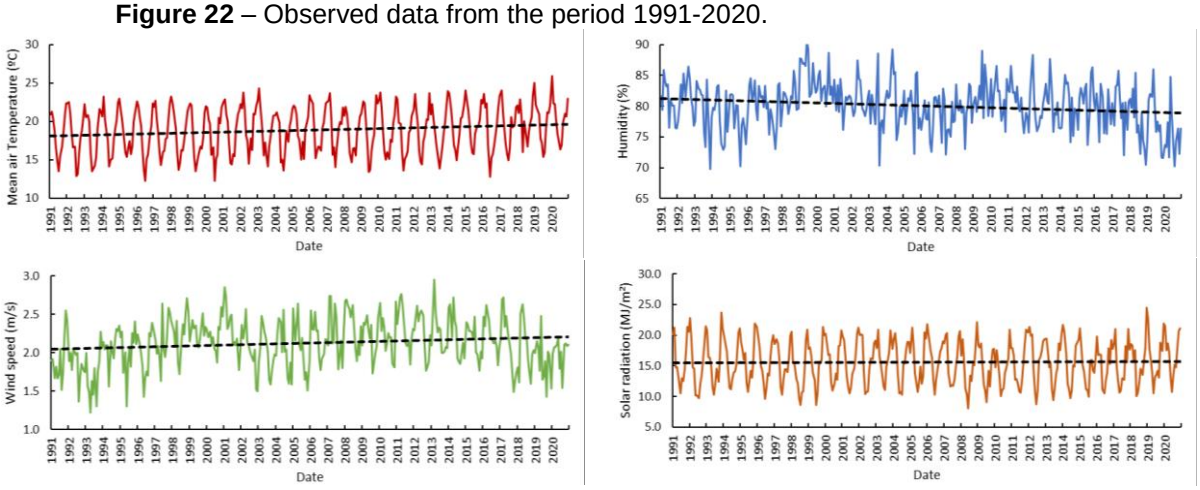

Note: Dashed line represents the trend over the period 1991-2020.
Source: The author.

5.3.2 Simulated scenarios (2040, 2060, 2080, and 2100)

PGECLIMA_R simulated meteorological data from both scenarios of the Sixth Assessment Report of the IPCC (2021), SSP1-1.9 and SSP5-8.5. The FAO Penman-Monteith method was used with the simulated data to estimate the evaporation rate. Figure 23 shows each year's annual evaporation and corresponding climate change scenario.

Figure 23 – Estimated evaporation for climate change scenarios.

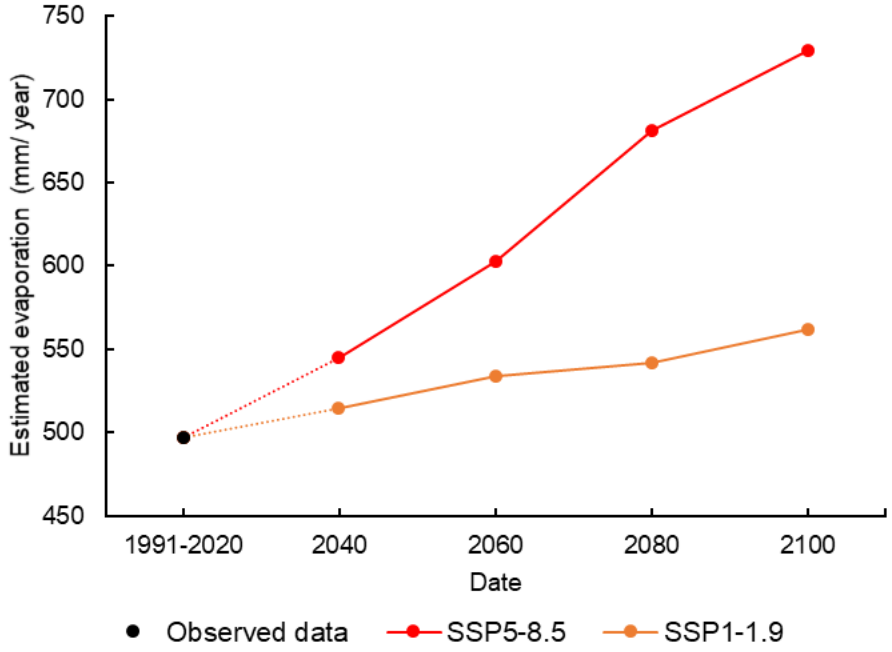

Source: The author.

An increase in the evaporation rates of 3.36%, 6.88%, 8.32%, and 11.59% is expected for the years 2040, 2060, 2080, and 2100 respectively, for the most optimistic scenario (SSP1-1.9), considering the temperature increase of 1.8 ºC by the end of 21st century. For the worst-case scenario (SPP5-8.5), considering the temperature increase of 5.7 ºC by the end of the 21st century, an increase in the evaporation rates of 8.76%, 17.50%, 27.06%, and 31.88% is expected for the years 2040, 2060, 2080, and 2100 respectively.

The current average annual evaporation of the Passaúna Reservoir is 496.56 mm year^{-1}. By 2100 an evaporation increase of 65.20 mm year^{-1} is expected for the optimistic scenario and 232.62 mm year^{-1} for the pessimistic scenario. Such values would result in annual evaporation of 562.14 mm year^{-1} and 729.57 mm year^{-1} for the SSP1-1.9 and SPP5-8.5 scenarios, respectively. Therefore, the evaporation rates would increase due to the climate change impacts.

Figure 24 presents the seasonal average daily evaporation in the climate change scenarios.

Figure 24 – Seasonal daily mean evaporation under climate change scenarios.

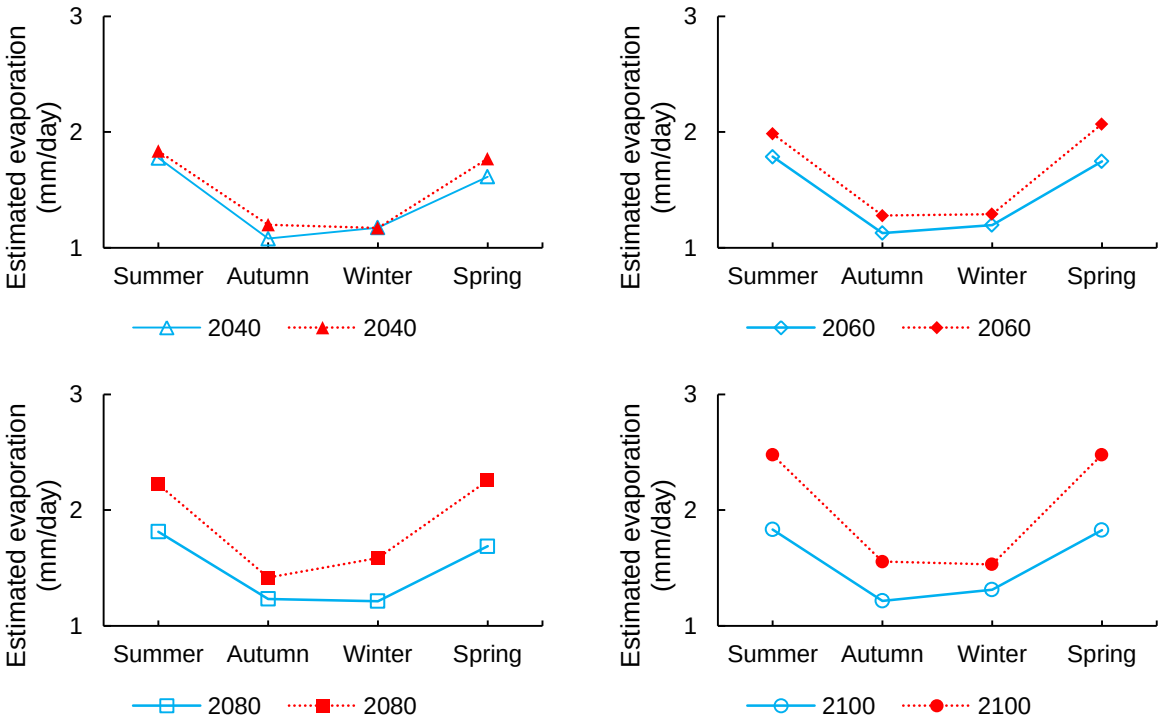

Note: Colors represent the scenarios: red - SPP5-8.5, blue - SPP1-1.9; Shapes represent the dates: triangles - 2040, diamonds - 2060, squares - 2080 and circles - 2100.
Source: The author.

As seen in Figure 24, summer and spring showed higher evaporation values in both scenarios. In all seasons, SSP5-8.5 presented higher values of average daily evaporation, except in the winter of 2040.

Similar values to our results were predicted for a reservoir in Australia, where an annual increase of 190 mm/year was found for 2070-2090 (HELFER; LEMCKERT; ZHANG, 2012). Differences could be due to different methods or scenarios to predict climate change.

Wang *et al.* (2018) also obtained results for a global evaluation of the effects of warmer climates on evaporation, where an increase between 250 and 350 mm/year is predicted for Brazil using IPCC scenario RCP 8.5 by 2100. Their result was slightly closer to our results, evaporation of 232.62 mm/year in 2100 for the SPP5-8.5 scenario.

5.3.3 FPS: efficiency in the water evaporation reduction

The efficiency in reducing evaporation from the FPS coverage area through the Assouline; Narkis; Or (2011) equation was 60.20%. It was used to calculate the volume of water saved by evaporation considering the FPS coverage area for the years 2040, 2060, 2080 and 2100 in the studied climate change scenarios.

As the FPS in the Passaúna Reservoir occupies a relatively small area in relation to the total size of the reservoir (0.01%), an FPS was assumed to occupy an area of 30% and 70% of the surface area of the reservoir. The Passauna reservoir has a total surface area of 8.5 km², so the areas covered by the FPS were 2.55 km² and 5.95 km².

Tables 5 and 6 show the estimated water volume saved with 30% and 70% of the Passaúna Reservoir area covered with the FPS for each climate change scenario.

Table 5 – Estimated evaporated volume without FPS and saved water volume with 30% of the Passaúna Reservoir area covered with floating photovoltaic system considering a total available surface area of 8.50 km².

Year	Evaporated volume without FPS (m^3 $year^{-1}$)	Estimated saved water volume with 30% area covered by FPS (m^3 $year^{-1}$)	Evaporated volume without FPS (m^3 $year^{-1}$)	Estimated saved water volume with 30% area covered by FPS (m^3 $year^{-1}$)
	SSP1-1.9	**SSP1-1.9**	**SSP5-8.5**	**SSP5-8.5**
2040	4,371,074.63	789,416.08	4,627,386.35	835,705.97
2060	4,534,738.26	818,973.73	5,124,244.13	925,438.49
2080	4,605,881.36	831,822.17	5,791,687.30	1,045,978.72
2100	4,778,270.65	862,955.68	6,201,358.06	1,119,965.26

Source: The author.

Table 6 – Estimated evaporated volume without FPS and saved water volume with 70% of the Passaúna Reservoir area covered with floating photovoltaic system considering a total available surface area of 8.50 km².

Year	Evaporated volume without FPS (m^3 $year^{-1}$)	Estimated saved water volume with 70% area covered by FPS (m^3 $year^{-1}$)	Evaporated Volume without FPS (m^3 $year^{-1}$)	Estimated saved water volume with 70% area covered by FPS (m^3 $year^{-1}$)
	SSP1-1.9	**SSP1-1.9**	**SSP5-8.5**	**SSP5-8.5**
2040	4,371,074.63	1,841,970.85	4,627,386.35	1,949,980.61
2060	4,534,738.26	1,910,938.70	5,124,244.13	2,159,356.48
2080	4,605,881.36	1,940,918.40	5,791,687.30	2,440,617.03
2100	4,778,270.65	2,013,563.25	6,201,358.06	2,613,252.29

Source: The author.

Based on the data shown in Tables 5 and 6, it was observed that the evaporated volume increased considerably between scenarios SPP1-1.9 and SSP5-8.5, especially in later years, with an increase of 5.86%, 12.99%, 25.74%, and 29.78% for the years 2040, 2060, 2080, and 2100 respectively.

In both scenarios, the FPS can prevent up to 18.06% of the evaporated volume by covering a surface area of 30% and 42.14% with 70% of the covered area, indicating that the evaporation reduction increases with more significant covered areas.

Lopes *et al.* (2020) studied the evaporation reduction efficiency by floating photovoltaic systems over the total reservoir area in the Brazilian semiarid region. Unevaporated water volumes per year of 21.2%, 37%, and 55.2% were obtained for covered areas of 30%, 50%, and 70%, respectively. The results showed that water savings by FPS installations would represent a reduction in annual government expenses of 13.38%, 14.36%, and 15.3% in water trucks for covered areas of 19.3%, 50%, and 70% (LOPES *et al.*, 2020).

Bontempo Scavo *et al.* (2020) obtained a 42% decrease in the evaporation for flexible modules, slightly in disagreement with the efficiency obtained of 60.20% by using Assouline; Narkis; Or (2011) methodology. Different approaches could explain such differences in obtaining the evaporation reduction efficiency of floating photovoltaic systems. Additionally, Bontempo Scavo *et al.* (2020) demonstrated that the greater the area covered by the FPS, avoiding exposure to the water surface, the greater the efficiency in the evaporation reduction by the covered areas.

5.4 CONCLUSION

The PGECLIMA_R software provided the results for the simulated climate change scenarios SPP1-1.9 and SPP5-8.5 predicted by the IPCC (2021). The FAO Penman-Monteith method was used from these results to obtain daily evaporation values for observed and simulated future climate change scenarios.

The meteorological database is essential to estimate reservoir evaporation rates, especially when direct measurements and historical data are unavailable, providing a way to predict the impacts of climate change.

The estimated evaporation increased 11.59% and 31.88% for the year 2100 in SPP1-1.9 and SPP5-8.5, respectively.

Water losses showed an increasing volume over the years by the end of the century, especially in later years, with a difference of 29.78% in the year 2100 between the optimistic and pessimistic scenarios. Considering an evaporation reduction efficiency of 60.20% by the coverage area of the floating photovoltaic system, 18.06% to 42.14% of water losses by evaporation can be prevented with a coverage area of 30% and 70%, respectively.

With the growing concern about climate change and its effects on water availability, the installation of floating photovoltaic systems in reservoirs can be a sustainable alternative to achieve a sustainable pathway, particularly in the future, and to provide efficient management of water resources.

FINAL CONSIDERATIONS

The effects of a floating photovoltaic system on a reservoir's evaporation rates are essential in evaluating its viability as a mitigation tool for reducing evaporation at present and in future climate change scenarios.

The first chapter presented a validation of methodologies to estimate evaporation rates through meteorological data in comparison with measured data of evaporation. The FAO Penman-Monteith (ALLEN *et al.*, 1998) and Linacre (1977) methods presented the best approximation to the direct measurements of evaporation obtained from the nearest weather station. In addition, it was also presented the efficiency in the evaporation reduction for the current floating photovoltaic system of 60.20% obtained by the Assouline; Narkis; Or method (2011). Later, it was simulated an expansion of the current FPS area to correspond to an energy production capacity of 1 MWp, 2.5 MWp and 5 MWp. The reduction of water evaporation for an area equivalent to an energy production capacity of 5 MWp would be enough to supply 196 people a year; therefore, greater areas would represent a valuable resource for managing water resources.

The second chapter presented the effects of the climate change on evaporation using IPCC climate change scenarios SSP1-1.9 and SSP5-8.5. Weather data were simulated from 30-year historical data. PGECLIMA_R simulated humidity, temperature, radiation variables and wind data through beta distribution. From the simulated data set, the FAO Penman-Monteith (ALLEN *et al.*, 1998) method was used to estimate the evaporation for the present scenario and the years 2040, 2060, 2080, and 2100. Furthermore, the influence of the floating photovoltaic system on the evaporation rates was investigated for 30% and 70% of the reservoir area covered. An increase in the evaporation of 31.88% compared to the present-day scenario was assessed in the SPP5-8.5 for the end of the century and 11.59% for the SPP1-1.9.

The region's greater values of evaporation occurred in the summer and spring. It was found that evaporated volume increased between scenarios SSP1-1.9 and SSP5-8.5, especially in later years, with an increase of 29.78% for 2100. Such effects of climate change can be prevented with the use of a floating photovoltaic system that can reduce from 18.06% up to 42.14% by covering 30% to 70% of the reservoir water surface area, respectively, representing volumes in the worst climate change scenario between 1.9 hm^3 to 2.6 hm^3.

The limitations of this research are due to the difficulty of obtaining measured evaporation data in the studied area, which was obtained in the nearest weather station to compare to the methods which used meteorological data from the study area. Demonstrating also the importance of such methods when measured data are unavailable locally, in which an approach through the meteorological data can be estimated. The study did not examine the different typologies of floating photovoltaic modules, energy production efficiency, and financial aspects of the FPS, which we recommend for future studies.

We highly recommend the installation of an experimental pilot plant in which different types of floating photovoltaic modules can be studied through direct evaporation measurements, providing more assertive values of their efficiencies in reducing evaporation and its effects.

Further studies can also lead to a better understanding of the effects of a floating photovoltaic system on the evaporation rates, especially with the availability of a greater set of data and new approaches to evaluation of the system.

Despite the limitations of this research, this preliminary approach to the effects of a floating photovoltaic system on the evaporation rates can contribute to future studies, especially considering that drought and climate change directly affect water availability resources. The water savings promoted by using a floating photovoltaic system can mitigate climate change impacts and be strategic for water resources management.

REFERENCES

ALLEN, R. G *et al.* **Crop evapotranspiration:** guidelines for computing crop water requirements. Rome: FAO, 1998. 300p. (FAO. Irrigation and Drainage Paper, 56).

ALTHOFF, D.; RODRIGUES, L. N.; DA SILVA, D. D. Impacts of climate change on the evaporation and availability of water in small reservoirs in the Brazilian savannah. **Climatic Change**, v. 159, p. 215–232, 2020. DOI: 10.1007/s10584-020-02656-y

ALVARES, C. A.; STAPE, J. L.; SENTELHAS, P. C.; GONÇALVES, J. L. D. M.; SPAROVEK, G. Köppen's climate classification map for Brazil. **Meteorologische Zeitschrift**, v. 22, n. 6, p. 711–728, 2013.

AMINZADEH, M.; LEHMANN, P.; OR, D. Evaporation suppression and energy balance of water reservoirs covered with self-assembling floating elements. **Hydrology and Earth System Sciences,** v. 22(7), p. 4015–4032. 2018. DOI: 10.5194/hess-22-4015-2018.

ANEEL - Agência Nacional de Energia Elétrica. Sistema de Informações de Geração (SIGA), 2022. Available from https://www.aneel.gov.br/siga. Access in: 26 mar. 2022.

ANEEL - Agência Nacional de Energia Elétrica. Resolução Normativa Nº 482, De 17 De Abril De 2012. Available from https://www.aneel.gov.br/. Access in: 26 mar. 2022.

ASSOULINE, S.; NARKIS, K.; OR, D. Evaporation from partially covered water surfaces. **Water Resources Research**, v. 46, n. 10, p. 1–12, 2010.

ASSOULINE, S.; NARKIS, K.; OR, D. Evaporation suppression from water reservoirs: Efficiency considerations of partial covers. **Water Resources Research**, v. 47, n. 7, p. 1–8, 2011.

BAI, H. *et al.* Assessing impacts of climate change and human activities on the abnormal correlation between actual evaporation and atmospheric evaporation demands in southeastern China. **Sustainable Cities and Society**, v. 56, n. September 2020, 102075, 2020.

BAZZI, H.; EBRAHIMI, H.; AMINNEJAD, B. A comprehensive statistical analysis of evaporation rates under climate change in Southern Iran using WEAP (Case study: Chahnimeh Reservoirs of Sistan Plain). **Ain Shams Engineering Journal**, 2020. DOI: https://doi.org/10.1016/j.asej.2020.08.030

BERUSKI, G. C. *et al.* Análise probabilística da velocidade média e caracterização da direção predominante do vento no município da lapa/pr. **Raega - O Espaço Geográfico em Análise**, [S.l.], v. 17, jun. 2009. ISSN 2177-2738. DOI: http://dx.doi.org/10.5380/raega.v17i0.11934.

BONTEMPO SCAVO, F.; Tina, G. M.; Gagliano, A.; Nižetić, S. An assessment study of evaporation rate models on a water basin with floating photovoltaic plants. **International Journal of Energy Research,** p. 1–22, 2020. DOI: https://doi.org/10.1002/er.5170.

BUENO, E. O. **Evaporação do reservatório da Usina Hidrelétrica de Camargos: caracterização da pegada hídrica.** Dissertação (Mestrado em Recursos Hídricos em Sistemas Agrícolas) – Universidade Federal de Lavras, 82 p., Lavras, MG, 2014.

BURGER, B. Public Net Electricity Generation in Germany 2020. Fraunhofer-Institute for Solar Energy Systems ISE. Germany, Freiburg. 2020. Available from https://www.ise.fraunhofer.de/content/dam/ise/en/documents/News/electricity_production_germany_2020.pdf. Acess on 19 Jan. 2021.

CAMARGO, A. P.; SENTELHAS, P. C. Avaliação do desempenho de diferentes métodos de estimativa da evapotranspiração potencial no estado de São Paulo**.** **Revista Brasileira de Agrometeorologia**, v.5, p.89-97, 1997.

CAMPOS LOPES, M. *et al.* Water-energy nexus: Floating photovoltaic systems promoting water security and energy generation in the semiarid region of Brazil. **Journal of Cleaner Production**, v. 273, 2020. DOI: https://doi.org/10.1016/j.jclepro.2020.122010

CARNEIRO, C.; KELDERMAN, P.; IRVINE, K. Assessment of phosphorus sediment-water exchange through water and mass budget in Passaúna Reservoir (Paraná

State, Brazil). **Environmental Earth Sciences**, 75:564, 2016. DOI: 1007/s12665-016-5349-3. Access on 22 Feb. 2021.

CARVALHO, L. G. de; DANTAS, A. A. A.; CASTRO NETO, P. **GNE 109**: Agrometeorologia. Lavras: Ed. UFLA, 2010. 184 p.

CAZZANIGA, R. *et al.* Floating photovoltaic plants: Performance analysis and design solutions. **Renewable and Sustainable Energy Reviews**, v. 81, n. September 2016, p. 1730–1741, 2018.

CIEL & TERRE INTERNATIONAL. **Floating Solar Plants References.** 2021. Available from https://www.ciel-et-terre.net/project_category/20-mwp/. Access on 08 Dec. 2021.

COELHO, C. D. *et al.* Estimates of monthly and annual evaporation rates and evaporated volumes per unit time in the Tucuruí-PA and Lajeado-TO hydroelectric power plant reservoirs based on different methods. **Eng. Agríc.**, Jaboticabal, v. 38, n. 1, p. 38-46, Jan. 2018. Available from http://www.scielo.br/scielo.php?script=sci_arttext&pid=S0100-69162018000100038&lng=en&nrm=iso. Access on 29 Jan. 2021.

COSTA, L. C. Dimensionamento de reservatórios para sistemas de abastecimento de água da chuva para a região dos campos gerais tendo em vista cenários de mudanças climáticas. 2016. 76 f. Dissertação (Mestrado em Saneamento Ambiental e Recursos Hídricos) - Universidade Estadual De Ponta Grossa, Ponta Grossa, 2016.

CRAIG, I. P. **Loss of storage water due to evaporation – a literature review**. National Centre for Engineering in Agriculture publication, University of Southern Queensland, Toowoomba, Australia. p.75. 2005b.

CRAIG, I.; GREEN, A.; SCOBIE, M.; SCHMIDT, E. **Controlling Evaporation Loss from Water Storages.** National Centre for Engineering in Agriculture Publication 1000580/1, University of Southern Queensland, Toowoomba, Australia. p. 207. 2005a.

CURTARELLI, M. P.; ALCÂNTARA, E. H.; ARAÚJO, C. A. S.; STECH, J. L.; LORENZZETTI, J. A. Avaliação da dinâmica temporal da evaporação no reservatório de Itumbiara, GO, utilizando dados obtidos por sensoriamento remoto. **Ambi-Agua**, Taubaté, v. 8, n. 1, p. 272-289, 2013. DOI: http://dx.doi.org/10.4136/ambiagua.1083.

DLOUHÁ, D.; DUBOVSKÝ, V.; POSPÍŠIL, L. Optimal calibration of evaporation models against penman–monteith equation. **Water (Switzerland),** v. 13, n. 11, 2021.

DONOHUE, R. J.; MCVICAR, T. R.; RODERICK, M. L. Assessing the ability of potential evaporation formulations to capture the dynamics in evaporative demand within a changing climate. **Journal of Hydrology**, v. 386, n. 1–4, p. 186–197, 2010.

EPE - Empresa de Pesquisa Energética. Balanço Energético Nacional (BEN) 2020: Ano base 2019. Available from https://ben.epe.gov.br. Access on 19 Jan. 2021.

EPE - Empresa de Pesquisa Energética. Anuário Estatístico De Energia Elétrica 2022: Ano base 2021. Available from https://epe.gov.br. Access on 15 Jul. 2021.

FALLS, L. W. The beta distribution: a statistical model for world cloud cover. Alabama, NASA, 1973, p.1-6. (NASA Tecnical Memorandum, TMX- 64714).

FAO and UN-Water. 2021. Progress on Level of Water Stress. Global status and acceleration needs for SDG Indicator 6.4.2, 2021. Rome. DOI: https://doi.org/10.4060/cb6241en

FLUMIGNAN, D. L. *et al.* Empirical methods for estimating reference surface net radiation from solar radiation. **Eng. Agríc.**, Jaboticabal, v. 38, n. 1, p. 32-37, Jan. 2018. Available from http://www.scielo.br/scielo.php?script=sci_arttext&pid=S0100-69162018000100032&lng=en&nrm=iso. Access on 07 Apr. 2021. DOI: https://doi.org/10.1590/1809-4430-eng.agric.v38n1p32-37/2018.

GOLYJESWSKI, O. W. **Simulation of thermal stratification using the a 2DV (CE-QUALW2) and a 3D (DELFT3D) mode. The case study: Passaúna Reservoir.** Dissertação (Mestrado em Engenharia Ambiental) - Universidade Federal do Paraná,

Setor de Tecnologia, Programa de Pós-Graduação em Engenharia Ambiental. Curitiba, p. 72. 2020. Available from https://www.prppg.ufpr.br/siga/visitante/trabalhoConclusaoWS?idpessoal=74668&idprograma=40001016075P3&anobase=2020&idtc=21. Access on 09 Feb. 2021.

GORJIAN, S. *et al.* Recent technical advancements, economics and environmental impacts of floating photovoltaic solar energy conversion systems. **Journal of Cleaner Production**, v. 278, p. 124285, 2021.

HAAS, J. *et al.* Floating photovoltaic plants: Ecological impacts versus hydropower operation flexibility. **Energy Conversion and Management**, v. 206, n. September 2019, 2020. DOI: https://doi.org/10.1016/j.enconman.2019.112414. Access on 29 Jan. 2021.

HARGREAVES, G. H.; SAMANI, Z. A. Reference crop evapotranspiration from temperature. **Applied Engineering in Agriculture**, v. 01, n. 02, p. 96-99, 1985.

HARTMANN, L. D. **Chapter 5 - The Hydrologic Cycle**. Global Physical Climatology: 2. Ed. Elsevier, 2016, p. 131-157. DOI: https://doi.org/10.1016/B978-0-12-328531-7.00005-0.

HARWELL, G. R. **Estimation of evaporation from open water**: A review of selected studies, summary of U.S. Army Corps of Engineers data collection and methods, and evaluation of two methods for estimation of evaporation from five reservoirs in Texas. U.S. Geological Survey Scientific Investigations Report 2012–5202, 96 p. 2012.

HASSAN, M. M. *et al.* Evaporation mitigation using floating modular devices. **Journal of Hydrology,** Elsevier, v. 530, p. 742–750, 2015. DOI: 10.1016/j.jhydrol.2015.10.027.

HELFER, F.; LEMCKERT, C.; ZHANG, H. Impacts of climate change on temperature and evaporation from a large reservoir in Australia**. Journal of Hydrology**, v. 475, p. 365–378, 19 Dec. 2012.

IPCC. **Climate Change 2014:** Synthesis Report. Contribution of Working Groups I, II and III to the Fifth Assessment Report of the Intergovernmental Panel on Climate Change [Core Writing Team, R.K. Pachauri and L.A. Meyer (eds.)]. IPCC, Geneva, Switzerland, 151 pp, 2014.

IPCC. **Climate Change 2021:** The Physical Science Basis. Contribution of Working Group I to the Sixth Assessment Report of the Intergovernmental Panel on Climate Change [Masson-Delmotte, V., P. Zhai, A. Pirani, S.L. Connors, C. Péan, S. Berger, N. Caud, Y. Chen, L. Goldfarb, M.I. Gomis, M. Huang, K. Leitzell, E. Lonnoy, J.B.R. Matthews, T.K. Maycock, T. Waterfield, O. Yelekçi, R. Yu, and B. Zhou (eds.)]. Cambridge University Press. In Press. 2021.

KOHLI, A.; FRENKEN, K., 2015. Evaporation from artificial lakes and reservoirs. FAO AQUASTAT Reports 10. Available from http://www.fao.org/3/a-bc814e.pdf. Access on 29 Jan. 2021.

LEITE, M.L.; VIRGENS FILHO, J.S.V. Avaliação da distribuição Beta com modelo probabilístico para análise de dados de velocidade do vento para Ponta Grossa – PR. **Publicatio UEPG**, Ciências Exatas e da Terra, Ciências Agrárias e Engenharias, Ponta Grossa, v. 23, n.1, p. 51-57, abril, 2007. DOI: https://doi.org/10.5212/publicatio.v13i01.879

LEITE, M.L.; VIRGENS FILHO, J.S.V. Avaliação da velocidade média e direção predominante do vento em Ponta Grossa – PR. **Revista Brasileira de Agrometeorologia**, Santa Maria, v.14, n. 2, p. 157-167, 2006.

LI, M. *et al.* Reference evapotranspiration variation analysis and its approaches evaluation of 13 empirical models in sub-humid and humid regions: A case study of the Huai River Basin, Eastern China. **Water (Switzerland),** v. 10, n. 4, p. 1–22, 2018.

LINACRE, E. T. A simple formula for estimating evaporation rates in various climates, using temperature data alone. **Agricultural Meteorology**, Amsterdam, v. 18, p. 409-424, 1977.

LINACRE, E. T. Data-sparse estimation of lake evaporation using a simplified Penman equation. **Agricultural and Forest Meteorology**, Elsevier, Amsterdam, v.64, n.3-4, p.237–256, 1993.

LIU, Q.; MCVICAR, T. R. Assessing climate change induced modification of Penman potential evaporation and runoff sensitivity in a large water-limited basin. **Journal of Hydrology**, v. 464–465, p. 352–362, 2012.

MAUÉS, J. A. Floating solar PV-hydroelectric power plants in Brazil: Energy storage solution with great application potential. **International Journal of Energy Production and Management**, v. 4, n. 1, p. 40–52, 2019.

MCMAHON, T. A., PEEL, M. C., LOWE, L., SRIKANTHAN, R., and MCVICAR, T. R. Estimating actual, potential, reference crop and pan evaporation using standard meteorological data: a pragmatic synthesis. **Hydrol. Earth Syst. Sci.**, v. 17, p. 1331–1363, Apr. 2013. DOI: https://doi.org/10.5194/hess-17-1331-2013. Access on 29 Jan. 2021.

MONTEITH, J. L. Evaporation and environment. **Symposia of the Society for Experimental Biology**. 19, pp. 205-234, 1965.

NEVES, G. L. **Impacto das mudanças climáticas globais na disponibilidade hídrica do solo no estado do Paraná.** 2015. 91f. Dissertação (Mestrado em Engenharia Sanitária e Ambiental - Área de Concentração: Saneamento Ambiental e Recursos Hídricos), Universidade Estadual de Ponta Grossa. Ponta Grossa, 2015.

NOAA - National Centers for Environmental Information. **State of the Climate: Global Climate Report for Annual 2020.** Published online January 2021. Available from: https://www.ncdc.noaa.gov/sotc/global/202013. Access on 26 Mar. 2022.

OLIVEIRA, G. X. S. **Relações entre medidas de evaporação de superfícies de água livre por evaporímetros e estimativas por métodos meteorológicos em duas regiões do Estado de São Paulo.** 2009. Tese (Doutorado em Física do

Ambiente Agrícola) - Escola Superior de Agricultura Luiz de Queiroz, Universidade de São Paulo, Piracicaba, 2009. DOI: 10.11606/T.11.2009.tde-04082009-111344.

O'NEILL, B.C. *et al.* The roads ahead: Narratives for shared socioeconomic pathways describing world futures in the 21st century. **Global Environmental Change**, 42, p. 169-180, 2017. DOI: 10.1016/j.gloenvcha.2015.01.004

PENMAN, H. L. Natural evaporation from open water, bare soil and grass. **Proceedings of the Royal Society.** A – Series, London, v.193, p.120–145, 1948.

PEREIRA, E. B *et al.* Atlas Brasileiro de Energia Solar. 2.ed. São José dos Campos: INPE, 2017. 80p. DOI: http://doi.org/10.34024/978851700089.

PEREIRA, S. B. *et al.* Evaporação líquida no lago de Sobradinho e impactos no escoamento devido à construção do reservatório. **Revista Brasileira de Engenharia Agrícola e Ambiental**, v. 13, n. 3, p. 346–352, 2009. DOI: https://doi.org/10.1590/S1415-43662009000300018.

PEREIRA, S. B. **Evaporação no lago de Sobradinho e disponibilidade hídrica no rio São Francisco.** 2004. 105 f. Tese (Doutorado em Engenharia Agrícola) - Universidade Federal de Viçosa, Viçosa. 2004.

ROCHA, É. D. J. T. *et al.* Estimativa da Et o pelo modelo Penman-Monteith FAO com dados mínimos integrada a um Sistema de Informação Geográfica. **Rev. Ciênc. Agron.**, Fortaleza, v. 42, n. 1, p. 75-83, Mar. 2011. DOI: http://dx.doi.org/10.1590/S1806-66902011000100010.

RODRIGUES, I. S.; RAMALHO, G. L. B.; MEDEIROS, P. H. A. Potential of floating photovoltaic plant in a tropical reservoir in Brazil. **Journal of Environmental Planning and Management**, v. 63, n. 13, p. 1–24, 2020. DOI: https://doi.org/10.1080/09640568.2020.1719824. Access on 29 Jan. 2021.

ROHWER. C. Evaporation from free water surfaces. Technical Bulletin no. 271, U.S. Department of Agriculture, 1931.

RStudio Team (2020). RStudio: Integrated Development Environment for R. RStudio, PBC, Boston, Massachusetts. Available from < http://www.rstudio.com/>; Access on 22 Feb. 2021.

SACRAMENTO, E. M. D. *et al.* **Scenarios for use of floating photovoltaic plants in Brazilian reservoirs.** IET Renewable Power Generation, November 2015. DOI:10.1049/iet-rpg.2015.0120

SALES, G. G. N. **Water quality modeling in a subtropical water supply reservoir.** Dissertação (Mestrado em Engenharia Ambiental) - Universidade Federal do Paraná, Setor de Tecnologia, Programa de Pós-Graduação em Engenharia Ambiental. Curitiba, p. 88. 2020. Available from https://acervodigital.ufpr.br/bitstream/handle/1884/69368/R%20-%20D%20-%20GABRIELA%20GOMES%20NOGUEIRA%20SALES.pdf?sequence=1&isAllowed=y. Access on 09 Feb. 2021.

SANEPAR. **Plano Diretor SAIC: Sistema de Abastecimento de Água Integrado de Curitiba e Região Metropolitana.** Sanepar, Curitiba, Brazil. 2013. Available from http://site.sanepar.com.br/arquivos/saicplanodiretor.pdf. Access on 09 Feb. 2021.

SANEPAR. Ross, Bárbara Z. L., Possetti, Gustavo R. C., Gervasoni, Ronald (org). **Inovação para a sustentabilidade a serviço do saneamento ambiental:** trabalhos contemplados no Prêmio Sanepar de Tecnologias Sustentáveis e no Prêmio Inova Sanepar. Edição 2018. Curitiba: Sanepar, 2019. 120p.

SGARBOSSA, C. K. **Use of solar energy for electric power generation and water heating in sustainable buildings in the state of Parana-Brazil considering future scenarios of global climate change.** 2019. Dissertation (Postgraduate Program in Sanitary and Environmental Engineering) - State University of Ponta Grossa, Ponta Grossa, 2019.

SOTIRI, K. *et al.* Implementation of comparative detection approaches for the accurate assessment of sediment thickness and sediment volume in the Passaúna Reservoir. **Journal of Environmental Management**, v. 287, n. February, p. 112298, 2021.

SUNGROW. **Floating PV System Case.** 2021. Available from https://en.sungrowpower.com/. Access on 08 dec. 2021.

TABOADA, M. E. *et al.* Solar water heating system and photovoltaic floating cover to reduce evaporation: Experimental results and modeling. **Renewable Energy**, v. 105, p. 601–615, 2017. DOI: 10.1016/j.renene.2016.12.094.

TIEPOLO, G. M.; PEREIRA, E. B.; URBANETZ JR, J.; PEREIRA, S. V.; GONCALVES, A. R.; LIMA, F. J. L.; COSTA, R. S., ALVES, A. R. "Atlas de Energia Solar do Estado do Paraná". 1ªEdição. Curitiba: UTFPR, 2017. Available from http://www.atlassolarparana.com/. Access on 22 Jan. 2021.

TSUNETO, L.; VIRGENS FILHO, J. Rainwater harvesting system using alternative energy sources in climate change scenarios in the State of Parana - Brazil. **IOP Conference Series: Earth and Environmental Science**, v. 503, p. 12037, Jun. 2020.

VALADARES, Bruno Ude Todde Fonseca. **Uma metodologia sobre estratégias de gerenciamento de energia para usinas fotovoltaicas flutuantes instaladas sobre reservatórios de usinas hidrelétricas.** Dissertação (Programa de Pós-Graduação em Engenharia Mecânica) – Universidade Federal de Minas Gerais, Belo Horizonte, 2017.

VALIANTZAS, J.D. Simplified versions for the Penman evaporation equation using routine weather data. **Journal of Hydrology**, 331, 690-702. DOI: 10.1016/j.jhydrol.2006.06.012

VIEIRA, N. P. A. *et al.* Estimativa da evaporação nos reservatórios de Sobradinho e Três Marias usando diferentes modelos. **Eng. Agríc.**, Jaboticabal, v. 36, n. 3, p. 433-448, jun. 2016. DOI: http://dx.doi.org/10.1590/1809-4430-Eng.Agric.v36n3p433-448/2016. Access on 29 Jan. 2021.

VIRGENS FILHO, J. S. *et al.* Analysis of the accuracy of daily series of global solar radiation simulated by the weather generator PGECLIMA_R, in the State of Parana,

Brazil. **Revista Brasileira de Geografia Física**, [S.l.], v. 7, n. 1, p. 180-192, abr. 2014. ISSN 1984-2295. DOI: https://doi.org/10.5935/1984-2295.20140005.

VIRGENS FILHO, J. S.; OLIVEIRA, P. M.; LEITE, M. L.; TSUKAHARA, R. Y. **PGECLIMA_R: Gerador estocástico para simulação de cenários climáticos brasileiros. II – Automação da análise estatística e validação dos dados simulados.** In: XVII Congresso Brasileiro de Agrometeorologia, 2011b, Guarapari, Anais... Guaraparí, Sociedade Brasileira de Agrometeorologia, p.1-5.

VIRGENS FILHO, J.S.; FÉLIX, R.P.; LEITE, M.L.; TSUKAHARA, R.Y. **PGECLIMA_R: Gerador estocástico para simulação de cenários climáticos brasileiros. I – Desenvolvimento do gerenciador do banco de dados climáticos.** In: XVII Congresso Brasileiro de Agrometeorologia, 2011a, Guarapari, Anais... Guaraparí, Sociedade Brasileira de Agrometeorologia, p.1-5.

WANG, W. *et al.* Global lake evaporation accelerated by changes in surface energy allocation in a warmer climate. **Nature Geoscience**, 11(6), 410–414, 2018. DOI:10.1038/s41561-018-0114-8

WMO, World Meteorological Organization. 2021 State of Climate Services. WMO-No. 1278. 2021.

WURBS, R. A.; AYALA, R. A. Reservoir evaporation in Texas, USA. **Journal of Hydrology.** Elsevier, v. 510, p. 1-9. 2013. DOI: 10.1016/j.jhydrol.2013.12.011.

XIAMEN MIBET ENERGY CO. LTD. **Floating PV System**. Available from https://www.mbt-energy.com/products/floating-pv/2008171.html. Access on 22 Feb. 2021.

YAO, Xi; ZHANG, Hong; LEMCKERT, Charles; BROOK, Adam; SCHOUTEN, Peter. **Evaporation Reduction by Suspended and Floating Covers: Overview, Modelling and Efficiency.** 2010.